Edelweiss Applied Science and Technology
ISSN: 2576-8484
Vol. 8, No. 5, 406-428
2024
Publisher: Learning Gate
DOI: 10.55214/25768484.v8i5.1697

Thermoelectric generators versus photovoltaic solar panels: Power and cost analysis

Osama A. Marzouk
University of Buraimi, Al Buraimi, Post Code 512, Sultanate of Oman; osama.m@uob.edu.om (O.A.M.)

Abstract: In the current study, the concept of building a power plant using thermoelectric generator (TEG) modules is investigated, both technically and economically. The hypothesized thermoelectric generation power plant is a modular system, consisting of a large array of electrically connected thermoelectric generator units for generating clean electricity with-out greenhouse gas (GHG) emissions, noise, or hazardous solid wastes. The envisioned thermoelectric generation power plant (TEGPP) considered here is assumed to utilize solar radiation as a heat source, and water as a heat sink. The viability of such a concept is examined in the current study based on available specifications of a high-output thermo-electric generator module released in the market (TEG1-24111-6.0). Benchmarking is car-ried out considering a high-efficiency photovoltaic (PV) panel in the market (SunPower SPR-MAX3-400), assuming that it operates under standard solar radiation of 1,000 W, and with a standard panel temperature of 25 °C, causing it to give an output electric power of 400 W (DC or direct current). It is found that in order to have an electric power of a thermoelectric generator unit similar to that of a photovoltaic panel of equal surface area, the temperature at the hot side of the thermoelectric generator unit should be about 70 °C if the cold-side temperature is 30 °C. However; under this output power equiva-lence, the price of the thermoelectric generator unit is about 90 times that of a photovol-taic panel of equal size (based on prices of October 2023). At an elevated hot-side tem-perature of 300 °C for the thermoelectric generator unit (with the cold-side temperature being still 30 °C), the thermoelectric generator unit can generate electric power that is about 25 times the power generated by a photovoltaic panel of an equal geometric area. This big boost in the output power still does not counteract the large cost difference be-tween the thermoelectric generator technology and the photovoltaic technology, where the per-watt(electric) cost in the case of thermoelectric generators is 3.5 times its value in the case of photovoltaic panels. Thus, the TEG technology in its intensified generation mode is still relatively more expensive compared to the PV technology. The practical im-plications of the current study are excluding the thermoelectric generation (based on the Seebeck effect) concept from large-scale commercial power plants, and viewing thermoe-lectric generators as sources of small electric power for waste heat management or con-venient power sources for small mobile devices.
Keywords: *Photovoltaic, Seebeck; PV, Solar Panel, TEG, Thermoelectric Generator.*

1. Introduction

1.1. The Seebeck Effect

The Seebeck effect (or the Seebeck thermoelectric effect) is a phenomenon where a temperature difference between the two points of contact of two different metals forming a closed circuit causes the metals to display magnetic properties due to an induced electric field. In other words, a temperature difference can result in a voltage difference and a flow of electricity [1–10]. The Seebeck effect is a key principle in the branch of physics called thermoelectricity [11–14]. The phenomenon was discovered in 1821 by Thomas Johann Seebeck, an Estonian-German physicist who was born in 1770 in Tallinn, the

* Correspondence: osama.m@uob.edu.om

capital of Estonia (was part of the Russian Empire at that time) and died in 1831 in Berlin (was part of Prussia at that time) [15–18]. The opposite of the Seebeck effect is the Peltier effect (where a flow of electricity through an electric junction of two dissimilar materials can induce a temperature difference across that junction, leading to a transfer of heat), which was discovered by the Fench physicist Jean Charles Peltier in 1834 (about 13 years after the discovery of the Seebeck effect) [19–30].

Despite being weak, the Seebeck effect was successfully utilized in temperature measurements through sensor elements called thermocouples [31–34].

1.2. The Seebeck Coefficient

The Seebeck effect is quantitatively expressed by the Seebeck coefficient (α), which is a proportionality factor relating the resulting voltage difference (ΔV) to the applied temperature difference (ΔT), over a narrow range of temperature [35–44].

$$\alpha = -\Delta V / \Delta T = |\Delta V / \Delta T| \quad (1)$$

The Seebeck coefficient is generally a function of temperature [45–47]. The Seebeck coefficient tends to be very small for metals, with no metal having a value above 100 μV/K (at 300 K). Furthermore, most metals have a Seebeck coefficient magnitude below 10 μV/K [38].

1.3. Thermoelectric Generator (TEG) Modules

In order to upgrade the Seebeck effect for use as a power source, magnification is performed through adopting semiconductor materials instead of metals, and through the arrangement of many thermoelectric elements that are connected electrically in series while subject to a common temperature difference between two sides (hot side and cold side) [49]. This special design leads to a thermoelectric generator (TEG) module, which may be viewed as a portable direct current (DC) power source in the shape of a thick plate, driven by a temperature difference [50–67]. It has a positive wire and a negative wire serving as electric terminals for connection to an external electric load, or for building an array through parallel and/or series connections [68–71].

1.4. Demonstration of Previous Work by Others

Small TEG-based power units were already produced commercially. These units may have a power rating of 10 W, converting heat (such as waste heat from a wood stove or a dedicated flame of a camping gas canister) into direct current electricity (with 5 V or 12 V voltage levels) for low-power applications, such as lighting and charging mobile phones [72–74].

The use of TEG models for recycling waste heat was proposed in different applications such as combustion gases of an electric generator, rear sides of solar photovoltaic (PV) panels, industrial furnaces, combined heat and power (CHP) systems, and fuel cells [75–87].

Qasim et al. [88] used the term "TEG Panel" to refer to an array of mechanically assembled TEG modules, which are connected electrically in series and parallel in order to achieve a desired overall voltage difference. Their experimental TEG panel consisted of 150 TEG modules (stacked with a pattern of 15 × 10 modules). The goal of the TEG panel was to convert waste heat from solar-heated water into electricity. The hot-water pipe was the hot side for the TEG panel, while a cold-water pipe, carrying normal tap water was used for cooling. A maximum temperature difference of 42.35 °C was reached, at which the open-circuit voltage was 15.3 V. The reported maximum TEG panel efficiency was 2.1%.

Dashevsky et al. [89] considered the main disadvantage of TEG to be the low efficiency of thermoelectric commercial modules. They proposed a special design, which can achieve an efficiency of up to 15%. The current study considers a commercially available TEG design, whose highest energy conversion efficiency (heat to electricity) is about 6%.

Gharzi et al. [90] experimentally investigated the integration of concentrated solar power (CSP) parabolic trough collectors (PTC) with thermoelectric generators (TEG), to yield a hybrid solar system designated by the term (PTC-TEG). The PTC units had a single-axis solar tracking mechanism, such that these longitudinal curved units can change their tilt as the direction of incoming solar beams changes from the east to the west during the day, while remaining oriented parallel to the north-to-south lines. Their results suggest that the TEG electricity generation is not very sensitive to the pressure of the pressurized heat transfer fluid (HTF) used in the absorber tubes within the CSP system.

Ji et al. [91] performed a techno-economic analysis (TEA) for the thermoelectric generator (TEG) in comparison with the organic Rankine cycle (ORC) for heat sources at low temperatures. In their analysis; noise level, modularity, lifespan, net present value (NPV), internal rate of return (IRR), payback period (PBP), cost per watt ($/W), and levelized cost of electricity (LCOE) were covered. Among their conclusions, the ORC technology was found to be better for heat sources with temperatures between 80 °C and 120 °C. On the other hand, the TEG technology can become better under certain conditions, such as a drop in the material price to 0.5 $/g.

Liu et al. [92] integrated the thermoelectric generator (TEG) concept with the heat pipe (HP) concept, and proposed a hybrid (HP-TEG) thermal energy-conversion system. Their innovative design is aimed for use over the moon, through utilizing the lunar daytime and nighttime. They found that the maximum achievable energy conversion efficiency is 7.6% when the length of the thermoelectric leg is 2.7 mm. They also estimated that their proposed heat pipe-based thermoelectric generator system can produce 1.75 MJ total power output during the lunar night. Based on their mathematical model, the researchers recommend that the number of TEG stages to be four, as an optimum value such that the HP-TEG system can attain the highest energy conversion efficiency throughout the lunar daytime and nighttime.

Zhao et al. [93] performed an energy and exergy analysis for thermoelectric generators, with the aim of recovering energy from the hot exhaust (as waste gases) from internal combustion engines in automobiles, through an exhaust thermoelectric generator (ETEG). The ETEG consists of thermoelectric generator modules (TEGMs), a cold fluid heat exchanger (CFHX), and an exhaust heat exchanger (EHEX). They found that higher exhaust temperatures cause lower total exergy efficiency. They also found that increasing the exhaust flow rate by a factor of five led to an increase in the power generation capacity by a factor of nearly seven, with a small change in the exergy losses.

Gull et al. [94] adopted the computational fluid dynamics (CFD) approach, with experimental validation, for investigating the electric performance of different configurations of a TEG array, in order to determine performance metrics such as the load voltage, the electric current, and the energy conversion efficiency. In computational fluid dynamics, the governing equations for the fluid are mathematically transformed such that an approximate numerical solution can be obtained, possibly with the aid of one or more submoelds for estimating relevant fluid properties [95–122]. In their study, they used the COMSOL-Multiphysics software in their computational modeling, which is a commercial tool for numerically modeling a wide range of problems [123–132]. For heating, hot water was used, with a controllable temperature within the range from 27 °C to 42 °C. In addition, the volume flow of either heating water or cooling water was varied from 0.5 L/min to 2 L/min. Their study showed that the performance of the hydro-thermoelectric system is more affected by the temperature of the heating water than its flow rate.

Readers interested in more details about the principles of thermoelectricity, as well as the materials used in this technology, and its applications as electricity sources in extreme environments, in waste heat recovery for transportation and industrial processes, and in sensors and microelectronics can consult a review by Champier [133], and another review by Shah et al. [134].

1.5. Objectives and Contributions

This study investigates the capability of electrically assembling an array of thermoelectric generator modules so that they become a candidate for a power plant for large-scale electricity generation, in a similar way that many solar photovoltaic panels can be assembled as an array and act as a renewable energy power plant, where electricity can be generated as a large commercial scale [135–146]. The heat source is direct solar radiation, and water cooling is expected by utilizing a nearby natural body of water (such as a sea). The power rating of such a power plant may exceed 5 MW, and it is intended for utility-scale use rather than a proprietary single-consumer system. Such an imagined thermoelectric generation power plant (TEGPP) has several advantages, such as not having moving parts (solid state device); which eliminates requirements for lubrication, avoids noise, and improves reliability [147–153]. However, it should be noted that additional electric inverter units are needed to convert the DC (direct current) electricity into AC (alternating current) electricity, and they can have moving fans for cooling [154]. A thermoelectric generator (TEG) system can be classified as a clean alternative power source if its heat source does not cause greenhouse gas (GHG), particularly carbon dioxide, or polluting gases and particulate matter from fossil fuel combustion [155–172]. Such clean power sources include those utilizing solar radiation or waste heat [173–179]. This adds another environmental advantage for TEG systems over conventional fossil-fuel-based power plants, making a TEG-based power plant suitable for use within urban communities and smart cities, as well as for electrified transportation when both direct and indirect emissions are aimed to be eliminated [180–183]. In contrast with photovoltaic panels, TEG systems can produce electricity in the absence of direct solar radiation, provided that an alternative heating source becomes available. Despite these attractive features of TEG systems, they have a low energy conversion efficiency, leading to a small power output. This is a significant limitation in these direct heat-to-electricity units.

While the current study acknowledges the potential value of thermoelectric generator (TEG) modules in low-power applications, such as personal uses, and or for utilizing waste heat in existing industrial or automotive processes, its main objective is to provide a data-driven answer to the question of: Can thermoelectric generators be used for large-scale electricity generation as a commercial power plant? The contribution made by this study to the power sector and to the fields of sustainability and renewable energy is a specific quantification of the comparison between the performance of TEG as power generation units as compared to the more established solar photovoltaic (PV) panels.

2. Methods

The research conducted here is primarily based on the analysis of performance data for a high-power thermoelectric generator (TEG) module. This is followed by a comparison with the performance of a high-efficiency photovoltaic solar panel. Through this analysis of numerical performance metrics, a decision can be made regarding the relative potential of both renewable energy technologies.

The thermoelectric generator (TEG) module considered here is a candidate from which a TEGPP can be formed. This TEG module corresponds to a high-power model, which is TEG1-24111-6.0, produced by the Canadian manufacturer TECTEG, which is a division of the Thermal Electronics Corporation (TEC) [184].

For benchmarking, a high-efficiency photovoltaic solar panel is considered here for comparison with the TEG modules. This panel (SPR-MAX3-400) is the model Maxeon 3 by the American company SunPower, having a nominal power of 400 W. It has a nominal solar-to-electric energy conversion efficiency of 22.6%. The term “nominal” here refers to an industrial standard (STC or standard test condition) for reporting the performance parameters of photovoltaic panels, with an artificial environment having a perpendicular incoming radiation level of 1,000 W/m^2, a panel’s cells temperature of 25 °C, and a specific reference spectral distribution that is referred to as AM 1.5 (or air mass 1.5) [185–204].

For fair and meaningful interpretation, normalized performance metrics were derived, such that they are expressed per unit area or per unit electric power output [205–208]. Therefore, these derived values are not only easier to understand, but are also not very dependent on the actual scale of electricity generation, and are applicable across different energy generation technologies.

3. Results

3.1. TEG-Based Electricity Generation

Figure 1 has a view of the TEG1-24111-6.0 thermoelectric generator. Two electric wires are also shown at the bottom, for the positive and the negative (ground) terminals. Figures 2-5 demonstrate the performance curves for the matched load, the voltage difference, the current, and the matched-load output power, respectively; for the TEG1-24111-6.0 thermoelectric generator. All these figures were taken (with permission) for the data sheet of that thermoelectric generator [209]. A matched load is a load having an optimized electric resistance value that corresponds to the maximum output power [210–216].

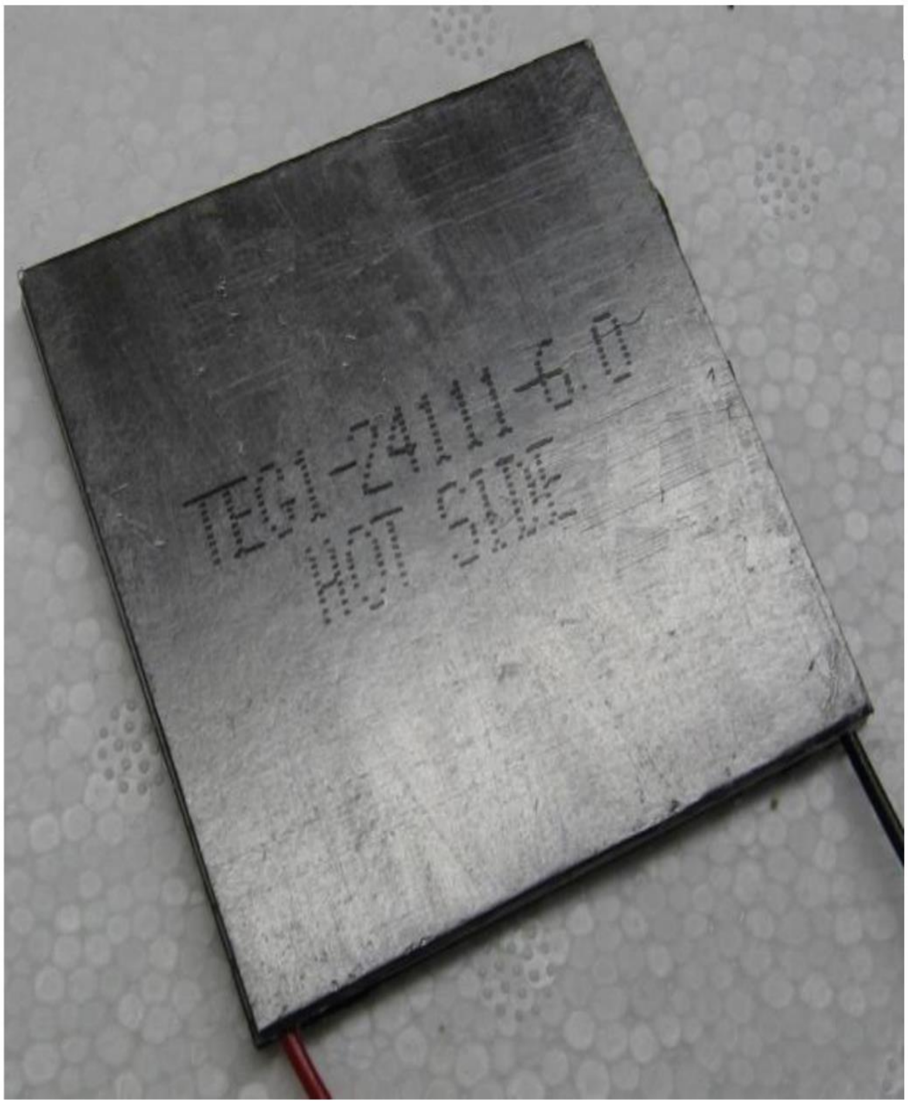

Figure 1.
A photo of the TEG1-24111-6.0 thermoelectric generator. The photo is taken from the product data sheet (used with permission).

DOI: 10.55214/25768484.v8i5.1697

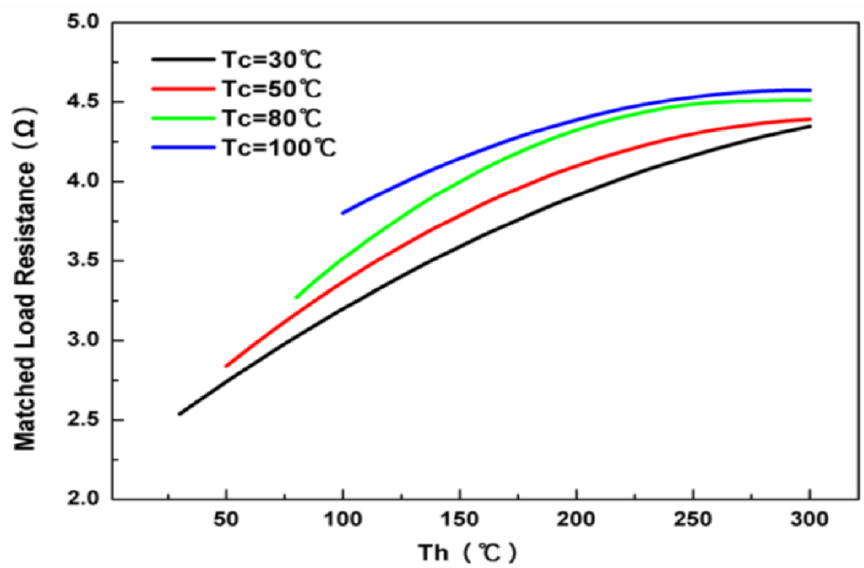

Figure 2.
The performance curves of the matched-load resistance versus the hot-side temperature (Th) for the TEG1-24111-6.0 thermoelectric generator. Each curve corresponds to a cold-side temperature (Tc).

The chart is taken from the product data sheet (Used with permission).

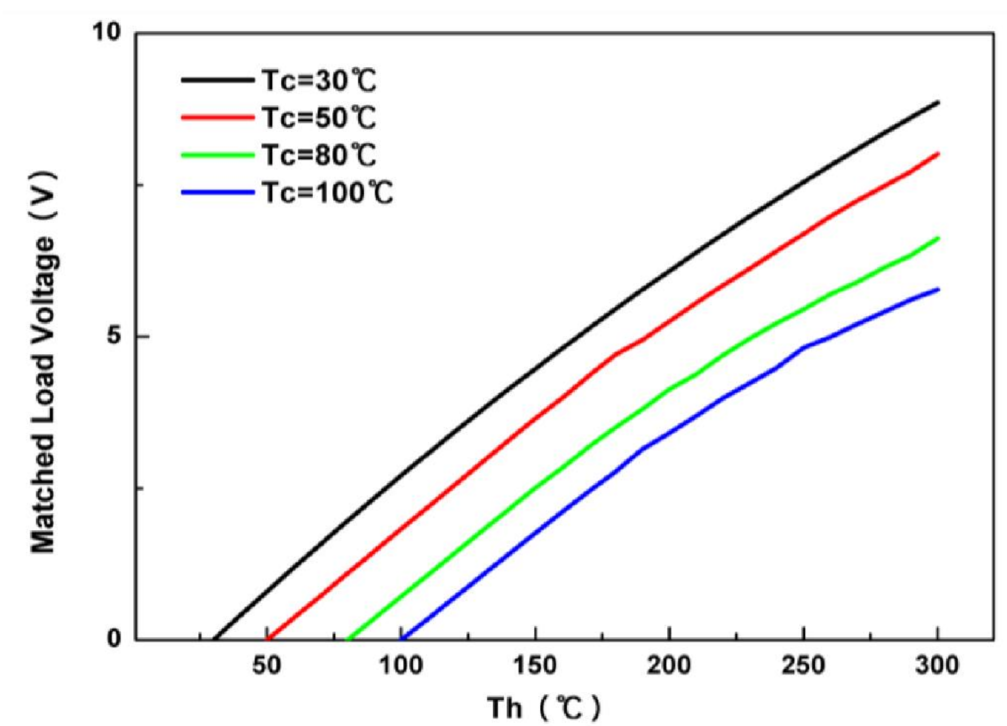

Figure 3.
The performance curves of the matched-load voltage difference versus the hot-side temperature (Th) for the TEG1-24111-6.0 thermoelectric generator. Each curve corresponds to a cold-side temperature (Tc).

The chart is taken from the product data sheet (used with permission).

Edelweiss Applied Science and Technology
ISSN: 2576-8484
Vol. 8, No. 5: 406-428, 2024
DOI: 10.55214/25768484.v8i5.1697

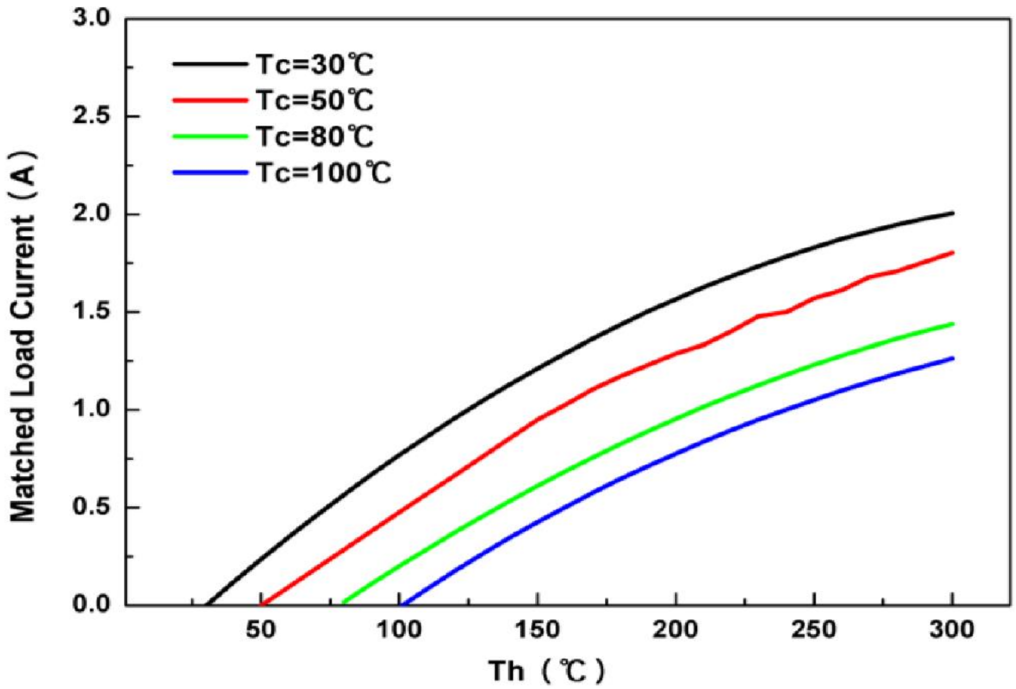

Figure 4.
The performance curves of the matched-load current versus the hot-side temperature (Th) for the TEG1-24111-6.0 thermoelectric generator. Each curve corresponds to a cold-side temperature (Tc).

The chart is taken from the product data sheet (used with permission).

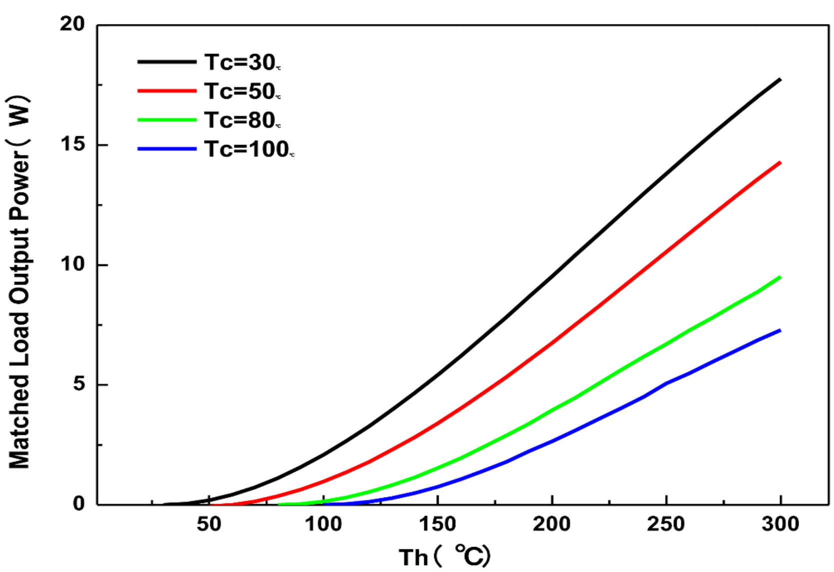

Figure 5.
The performance curves of the matched-load output power versus the hot-side temperature (Th) for the TEG1-24111-6.0 thermoelectric generator. Each curve corresponds to a cold-side temperature (Tc).

Edelweiss Applied Science and Technology
ISSN: 2576-8484
Vol. 8, No. 5: 406-428, 2024
DOI: 10.55214/25768484.v8i5.1697

The chart is taken from the product data sheet (used with permission).
Table 1 provides a summary of some conditions for the TEG module as well as selected operational conditions for the TEGPP.

Table 1.
Settings for the thermoelectric generator (TEG1-24111-6.0), as a possible module in a TEGPP.

Setting	Type	Value
Cold side temperature	Assumption	30 °C
Hot side temperature	Assumption	70 °C
Power mode	Assumption	Matched load (Maximum power)
Load resistance	Performance curve	2.9 Ω (Approximately)
Voltage difference	Performance curve	1.4 V (Approximately)
Electric current	Calculated (Voltage difference ÷ load resistance, with performance curve validation)	0.48 A
Module power	Calculated (Voltage difference × Electric current, with performance curve validation)	0.672 W
Dimensions	Data sheet	0.056 m × 0.056 m
Module area	Calculated (module length × module width)	0.003136 m^2
Power density	Calculated (Module power ÷ module area)	214.3 W/m^2
Modules per m^2	Calculated (1 m^2 ÷ module area)	318.878
Price per module	Online, by manufacturer	USD 54.00
Cost per m^2 of modules	Calculated (Price per module ÷ module area)	17,219.4 USD/m^2
Cost per W of output	Calculated (price per module ÷ module power)	80.3571 USD/W

The following formulas were used to obtain the derived (computed rather than assumed or taken from the manufacturer's performance curve) parameters of the thermoelectric generator that are listed in the above table [217–220]:

$$\text{Electric current} = \text{Voltage difference} / \text{Load resistance} \quad (2)$$

$$\text{Module power} = \text{Voltage difference} \times \text{Electric current} \quad (3)$$

The module power can also be estimated as

$$\text{Module power} = (\text{Voltage difference})^2 / \text{Load resistance} \quad (4)$$

$$\text{Module area} = \text{Module length} \times \text{Module width} \quad (5)$$

$$\text{Number of modules per square meter} = \text{Unit area} / \text{Module area} \quad (6)$$

$$\text{Cost per square meter of modules} = \text{Price of one module} / \text{Module area} \quad (7)$$

$$\text{Cost per power output} = \text{Price of one module} / \text{Power output from one module} \quad (8)$$

The TEG module price (USD 54.00) listed in the previous table reflects a discount for bulk orders (buying between 50 and 99 TEG modules). For the smallest orders (from 1 to 9 TEG modules), the price increases to USD 58.00, leading to a higher price of 18,494.9 USD /m^2 when a standardized 1 m^2 of generating surface is considered.

In the above table, the TEG module area of 0.003136 m^2 is the result of multiplying the length of the TEG module by its width. Since the particular TEG module considered here has a square shape, its width and length are equal. Thus, the module area is effectively the squared value of its side length, which is 0.056 m. The module power of 0.672 W is computed as the product of the electric current (0.48 A) and the voltage difference (1.4 V), based on a fundamental rule in electric power systems and electronics [221]. The power density is a term used here to refer to the DC electric power output per unit area of modules. It is computed by dividing the electric power from one TEG module by the area of that TEG module. This quantity is analogous to the quantity "heat flux" or "heat flow density" in the field of heat transfer, but it refers to an electric power rather than a thermal power [222]. The quantity (modules per m²) means the number of TEG modules that can be placed next to each other (vertically and horizontally) such that they fill an area of 1 m². This value is theoretical, and does not need to be an integer value. It is obtained by dividing the reference area of a square meter (1 m²) area by the area of one TEG module.

In the above table, the quantity (cost per m² of modules) is the cost of the estimated number of TEG modules needed to fill a theoretical reference area of 1 m². Therefore, this quantity is computed as the product of the quantity (modules per m²) and the quantity (price per module). The quantity (cost per W of output) is an estimate of the cost of one electric power unit (one watt or 1 W) using the considered TEG module. It is computed by dividing the quantity (price per module) by the quantity (module power). In the current study, this means dividing (USD 54.00) by (0.672 W), which gives (80.3571 USD/W).

3.1. PV-Based Electricity Generation

It becomes very useful to establish a reference power generation option, such that the TEG option presented earlier can be contrasted with it, as a benchmarking level to compare with [223–226]. The selected reference electricity generation technology here is solar photovoltaic (PV) panels, which represent a mature and widely utilized method for generating electricity in a clean way, with flexibility in the system size, and without harmful emissions [227–233]. The PV power capacity is expected to increase significantly until 2050, as an attempt to reduce the dependence of the energy sector on fossil fuels [234,235].

Table 2 lists some features of a benchmarking PV panel (SPR-MAX3-400), based on the manufacturer's data sheet and the selling price provided by an online supplier [236].

Table 2.
Settings of the SunPower Maxeon 3 solar photovoltaic panel (SPR-MAX3-400).

Setting	Type	Value
Power mode	Assumption	Standard test condition (1,000 W/m² solar radiation, 25 °C panel temperature), and maximum power
Voltage difference	Data sheet	65.8 V
Current	Data sheet	6.08 A
Panel power	Calculated (Voltage difference × electric current, with data sheet validation)	400 W
Dimensions	Data sheet	1.690 m × 1.046 m
Panel area	Calculated (Panel length × panel width)	1.76774 m²
Power density	Calculated (Panel power ÷ panel area)	226.3 W/m²
Energy efficiency	Calculated (Power density ÷ standard solar radiation value, with data sheet validation)	22.6%
Panels per m²	Calculated (1 m² ÷ panel area)	0.565694
Price per panel	Online, by a European supplier (in Lithuania)	EUR 335.00 (Equivalent to USD 353.38 as of

Setting	Type	Value
		18/October/2023)
Cost per m² of panels	Calculated (Price per panel ÷ panel area)	199.90 USD/m²
Cost per W of output	Calculated (Price per panel ÷ panel power)	0.88345 USD/W

The following formulas were used to obtain the derived (computed rather than assumed or taken from the manufacturer's performance curve) parameters of the thermoelectric generator that are listed in the above table [237–240]:

$$\text{Panel output electric power} = \text{Voltage difference} \times \text{Electric current} \quad (9)$$

$$\text{Panel area} = \text{Panel length} \times \text{Panel width} \quad (10)$$

$$\text{Panel power density} = \text{Panel output electric power} \div \text{Panel area} \quad (11)$$

$$\text{Energy efficiency (solar-to-electric)} = \text{Panel power density} / \text{Standard solar radiation value} \quad (12)$$

$$\text{Number of panels per square meter} = \text{Unit area} / \text{Panel area} \quad (13)$$

$$\text{Cost per square meter of panels} = \text{Price of one module} / \text{Module area} \quad (14)$$

$$\text{Cost per power output} = \text{Price of one panel} / \text{Power output from one panel} \quad (15)$$

The PV panel price (EUR 335.00, equivalent to USD 353.38 as of 18/October/2023) listed in the previous table reflects a discount for bulk orders (when buying 100 PV panels). For the smallest orders (less than 20 PV panels), the price increases to EUR 346.00 (equivalent to USD 365.01 as of 18/October/2023), leading to a higher price of 206.48 USD/m² when a standardized 1 m² of generating surface is considered.

4. Discussion

The analysis in the previous section suggests that the TEG modules and the PV panels can give similar DC electric power output per unit surface area under their optimized operations. When comparing 214.3 W/m² for the TEG module with 226.3 W/m² for the PV panel, the magnitude of the relative difference is below 6%.

However, the cost of power is significantly different for the two technologies. The cost of a unit power in the case of the TEG technology is about 91.0 times its value for the PV technology (80.3571 USD/W compared to 0.88345 USD/W). This does not even take into account the added expenses of the cooling system for the TEG modules.

The manufacturer of the investigated TEG module has a recommended operational condition of 30 °C for the cold side, and 300 °C for the hot side (which is near the maximum allowed limit of 320 °C). In that intense mode, the heat flow density across the module is about 96,000 W/m², which is 96 times the standard solar radiation power of 1,000 W/m². This is an enormous heating requirement, which also demands excessive cooling at the cold side of the TEG module.

The electric power density (with a matched load) under this TEG intense condition is 5,612.2 W/m² (computed as 17.6 W/module ÷ 0.003136/module). This is 24.8 times the power density of a PV panel under its standard condition (which is 226.3 W/m²). With a needed heat flow density of 96,000 W/m², the heat-to-electricity conversion efficiency for the TEG module in that case is only 5.85% or 0.0585 (computed as 5,612.2 W(electric)/m² ÷ 96,000 W(thermal)/m²).

The estimated cost per watt under such an intense TEG operation drops by a factor of 26.19, from 80.3571 USD/W (computed as 54.00 USD/module ÷ 0.672 W/module) to 3.06818 USD/W (computed as 54.00 USD/module ÷ 17.6 W/module). Despite this big decline, this cost per unit power (3.06818 USD/W) is still 3.47 times higher than the estimated one for PV panels (which is 0.88345 USD/W).

5. Conclusions and Possible Future Work

5.1. Concluding Remarks

A thermoelectric generator (TEG) is a solid-state semiconductor device that produces a direct current voltage when subject to a temperature difference, through a phenomenon known as the Seebeck effect. The thermoelectric generator technology has been proposed for waste heat recovery, through generating electricity from a source of heat that is not otherwise exploited, such as the hot exhaust gas released from a vehicle engine.

Based on an assessment of the power generation capability and its economic aspect, this study concludes that a thermoelectric generation power plant (TEGPP) is far from being realistic. Such a TEGPP cannot compete with a solar photovoltaic power plant, primarily due to the large cost gap that cannot be bridged by intensifying the operational conditions to a level near the maximum allowed temperature. However, thermoelectric generators (TEG) are still successful in energy harvesting through converting waste heat into useful electricity.

At moderate operating conditions (standard solar radiation of 1,000 W/m^2 for solar panels and a temperature difference of 40 °C for thermoelectric generators), the electric output power density (electric output power per unit area) for both electric power generation technologies becomes comparable, but the cost of a unit power using thermoelectric generators is about two orders of magnitude greater than its counterpart using photovoltaic solar panels. If the temperature difference for thermoelectric generators is boosted by a factor of about eight (from 40 °C to 270 °C), the electric output power density using thermoelectric generators surpasses well (roughly 25 times) that of solar panels, but the heat-to-electricity conversion efficiency with thermoelectric generators in such an exceptional case remains relatively very low (nearly 6% only) compared to what photovoltaic solar panels may achieve under ordinary sunlight, with a solar-to-electric power conversion efficiency around 23%, thus roughly four times better than what thermoelectric generators can achieve with intensified operation (which can require sophisticated systems for both heating and cooling).

In summary, thermoelectric generators are successful in supplying electricity to low-power loads (a few watts) directly from a source of heat that can be conveniently portable, or in producing electricity from an existing source of waste heat. On the other hand, thermoelectric generators are not yet feasible choices for large power generation systems.

5.2. Possible Research Extension

A thermoelectric generator (TEG) is a solid-state semiconductor device that produces a direct current voltage when subject to a temperature difference, through a phenomenon known as the Seebeck effect. The thermoelectric generator technology has been proposed for waste heat recovery, through generating electricity from a source of heat that is not otherwise exploited, such as the hot exhaust gas released from a vehicle engine.

The work presented in the current study may be extended by exploring special configurations in which a thermoelectric generation power plant (TEGPP) becomes justifiable, through utilizing existing resources or environmental factors that boost the performance of such an imagined source of green (emissions-free) electricity. For example, the combination of TEG modules with flat concentrated solar power (CSP) surfaces may enable a dual-mode power plant, where the CSP elements (such as heliostat mirrors or linear Fresnel reflectors) take their input heat through direct solar radiation, whereas the flat TEG modules take their input heat indirectly from the hot rear faces of the CSP (not the radiation-collector faces) [241–261]. Thus, the CSP system constitutes a higher-temperature stage, whereas the TEG system constitutes a lower-temperature stage. The overall electricity output is the sum of generated electricity (direct current) from both stages. In addition, effective cooling (air-based or liquid-based, passive/natural or active/forced) should then be considered carefully to maximize the temperature difference between the hotter side and the colder side of the TEG modules.

Another scenario for TEG utilization is the combination with geothermal energy, as an attractive renewable energy source and a massive natural source of stored heat beneath the surface of the earth .

Acknowledgement:
Gerard Campeau (CEO, Thermal Electronics Corp. - TEC) for granting the author a permission to reproduce images from the data sheet of the company's thermoelectric generator module (TEG1-24111-6.0) http://www.thermoelectric-generator.com for non-commercial purposes. This module was beneficially used in the current study.

References

[1] M. Wang, C. Bi, L. Li, S. Long, Q. Liu, H. Lv, N. Lu, P. Sun, M. Liu, Thermoelectric Seebeck effect in oxide-based resistive switching memory, Nat. Commun. 5 (2014) 4598. https://doi.org/10.1038/ncomms5598.
[2] O. Nickel, L.J.V. Ahrens-Iwers, R.H. Meißner, M. Janssen, Water, Not Salt, Causes Most of the Seebeck Effect of Nonisothermal Aqueous Electrolytes, Phys. Rev. Lett. 132 (2024) 186201. https://doi.org/10.1103/PhysRevLett.132.186201.
[3] Z. Li, J. Jiang, X. He, C. Wang, Y. Niu, Recent progress on the thermoelectric effect for electrochemistry, J. Mater. Chem. A 12 (2024) 13623–13646. https://doi.org/10.1039/D4TA00256C.
[4] M. Sajdak, J. Tobola, T. Parashchuk, M. Krzywiecki, P. Powroźnik, K.T. Wojciechowski, Probing hydrogen content in steel using the thermoelectric effect, Chem. Eng. J. 485 (2024) 149735. https://doi.org/10.1016/j.cej.2024.149735.
[5] M. Parzer, T. Schmid, F. Garmroudi, A. Riss, T. Mori, E. Bauer, Measurement setup for Nernst and Seebeck effect at high temperatures and magnetic fields tested on elemental bismuth and full-Heusler compounds, Rev. Sci. Instrum. 95 (2024) 043906. https://doi.org/10.1063/5.0195486.
[6] Y. Suzumura, T. Tsumuraya, M. Ogata, Seebeck Effect of Dirac Electrons in Organic Conductors under Hydrostatic Pressure Using a Tight-Binding Model Derived from First Principles, J. Phys. Soc. Jpn. 93 (2024) 054704. https://doi.org/10.7566/JPSJ.93.054704.
[7] Inamuddin, T. Altalhi, M.A.J. Mazumder, THERMOELECTRIC POLYMERS: properties and applications, MATERIALS RESEARCH FORUM, MILLERSVILLE, 2024.
[8] J. Jang, J.W. Jo, T. Ohto, H.J. Yoon, Seebeck Effect in Molecular Wires Facilitating Long-Range Transport, J. Am. Chem. Soc. 146 (2024) 4922–4929. https://doi.org/10.1021/jacs.3c14012.
[9] Y. Kimura, K. Utsumi, H. Tohmyoh, Experimental relationship between the Seebeck and Peltier effects in thermoelectric modules based on Fe and Al metals, Appl. Therm. Eng. 255 (2024) 124009. https://doi.org/10.1016/j.applthermaleng.2024.124009.
[10] H. Arisawa, Y. Fujimoto, T. Kikkawa, E. Saitoh, Observation of nonlinear thermoelectric effect in MoGe/$Y_3Fe_5O_{12}$, Nat. Commun. 15 (2024) 6912. https://doi.org/10.1038/s41467-024-50115-4.
[11] E. Grodzinsky, M. Sund Levander, History of the Thermometer, in: E. Grodzinsky, M. Sund Levander (Eds.), Underst. Fever Body Temp., Springer International Publishing, Cham, 2020: pp. 23–35. https://doi.org/10.1007/978-3-030-21886-7_3.
[12] K. Behnia, Fundamentals of thermoelectricity, Oxford University Press, Oxford, United Kingdom, 2015.
[13] D.K.C. MacDonald, Thermoelectricity: an Introduction to the Principles, Dover Publications, 2013.
[14] I. Terasaki, Introduction to thermoelectricity, in: Mater. Energy Convers. Devices, Elsevier, 2005: pp. 339–357. https://doi.org/10.1533/9781845690915.3.339.
[15] E. Velmre, Thomas Johann Seebeck and his contribution to the modern science and technology, in: 2010 12th Bienn. Balt. Electron. Conf., IEEE, Tallinn, Estonia, 2010: pp. 17–24. https://doi.org/10.1109/BEC.2010.5631216.
[16] Encyclopedia Britannica, Thomas Johann Seebeck, (n.d.). https://www.britannica.com/print/article/532353 (accessed October 8, 2022).
[17] K. Behnia, What is measured when measuring a thermoelectric coefficient?, Comptes Rendus Phys. 23 (2023) 25–40. https://doi.org/10.5802/crphys.100.
[18] M.A. Qasim, V.I. Velkin, A.K. Hassan, Seebeck Generators and Their Performance in Generating Electricity, J. Oper. Autom. Power Eng. (2022). https://doi.org/10.22098/joape.2022.9715.1677.
[19] M. Leone, History of Physics as a Tool to Detect the Conceptual Difficulties Experienced by Students: The Case of Simple Electric Circuits in Primary Education, Sci. Educ. 23 (2014) 923–953. https://doi.org/10.1007/s11191-014-9676-z.
[20] Z. Slanina, M. Uhlik, V. Sladecek, Cooling Device with Peltier Element for Medical Applications, IFAC-Pap. 51 (2018) 54–59. https://doi.org/10.1016/j.ifacol.2018.07.129.
[21] D. González-Mendizabal, P. Bortot, A.L.L. De Ramos, A Thermal Conductivity Experimental Method Based on the Peltier Effect, Int. J. Thermophys. 19 (1998) 1229–1238. https://doi.org/10.1023/A:1022610330376.
[22] J. Flipse, F.L. Bakker, A. Slachter, F.K. Dejene, B.J. Van Wees, Direct observation of the spin-dependent Peltier effect, Nat. Nanotechnol. 7 (2012) 166–168. https://doi.org/10.1038/nnano.2012.2.

[23] V.A. Drebushchak, The Peltier effect, J. Therm. Anal. Calorim. 91 (2008) 311–315. https://doi.org/10.1007/s10973-007-8336-9.
[24] E. Edlund, XXXI. *On the cause of the phenomena of voltaic cooling and heating discovered by* Peltier, Lond. Edinb. Dublin Philos. Mag. J. Sci. 38 (1869) 263–268. https://doi.org/10.1080/14786446908641339.
[25] K. Uchida, S. Daimon, R. Iguchi, E. Saitoh, Observation of anisotropic magneto-Peltier effect in nickel, Nature 558 (2018) 95–99. https://doi.org/10.1038/s41586-018-0143-x.
[26] H. Najafi, K.A. Woodbury, Optimization of a cooling system based on Peltier effect for photovoltaic cells, Sol. Energy 91 (2013) 152–160. https://doi.org/10.1016/j.solener.2013.01.026.
[27] F.L. Bakker, A. Slachter, J.-P. Adam, B.J. Van Wees, Interplay of Peltier and Seebeck Effects in Nanoscale Nonlocal Spin Valves, Phys. Rev. Lett. 105 (2010) 136601. https://doi.org/10.1103/PhysRevLett.105.136601.
[28] S. Kodeeswaran, T. Ramkumar, R.J. Ganesh, Precise temperature control using reverse seebeck effect, in: 2017 Int. Conf. Power Embed. Drive Control ICPEDC, IEEE, Chennai, India, 2017: pp. 398–404. https://doi.org/10.1109/ICPEDC.2017.8081122.
[29] M.K. Rathod, J.R. Patel, A novel cooling strategy for lithium-ion battery thermal management with phase change material, in: Handb. Therm. Manag. Syst., Elsevier, 2023: pp. 309–322. https://doi.org/10.1016/B978-0-443-19017-9.00036-2.
[30] A. Uysal, A. Keçebaş, M. Kayfeci, Futuristic methods of electronics cooling, in: Handb. Therm. Manag. Syst., Elsevier, 2023: pp. 687–702. https://doi.org/10.1016/B978-0-443-19017-9.00026-X.
[31] L. Huang, J. Chen, Z. Yu, D. Tang, Self-Powered Temperature Sensor with Seebeck Effect Transduction for Photothermal–Thermoelectric Coupled Immunoassay, Anal. Chem. 92 (2020) 2809–2814. https://doi.org/10.1021/acs.analchem.9b05218.
[32] A.W. Van Herwaarden, P.M. Sarro, Thermal sensors based on the seebeck effect, Sens. Actuators 10 (1986) 321–346. https://doi.org/10.1016/0250-6874(86)80053-1.
[33] F. Reverter, A Tutorial on Thermal Sensors in the 200th Anniversary of the Seebeck Effect, IEEE Sens. J. 21 (2021) 22122–22132. https://doi.org/10.1109/JSEN.2021.3105546.
[34] A.V. Karpov, A.E. Sytschev, A.O. Sivakova, Device for measurement the seebeck coefficient of thermoelectric materials in the temperature range 300–800 K, Meas. Tech. 66 (2023) 628–635. https://doi.org/10.1007/s11018-023-02275-w.
[35] A.I. Hofmann, R. Kroon, C. Müller, Doping and processing of organic semiconductors for plastic thermoelectrics, in: Handb. Org. Mater. Electron. Photonic Devices, Elsevier, 2019: pp. 429–449. https://doi.org/10.1016/B978-0-08-102284-9.00013-9.
[36] L. Wang, X. Zhang, L.-D. Zhao, Evolving Strategies Toward Seebeck Coefficient Enhancement, Acc. Mater. Res. 4 (2023) 448–456. https://doi.org/10.1021/accountsmr.3c00009.
[37] P.K. Rawat, B. Paul, Simple design for Seebeck measurement of bulk sample by 2-probe method concurrently with electrical resistivity by 4-probe method in the temperature range 300–1000 K, Measurement 91 (2016) 613–619. https://doi.org/10.1016/j.measurement.2016.05.104.
[38] C. Li, C. Shan, D. Luo, X. Gu, Q. Le, A.K.K. Kyaw, Z. Dong, K. Sun, J. Ouyang, Great Enhancement in the Seebeck Coefficient of PEDOT:PSS by Polaron Level Splitting via π–π Overlapping with Nonpolar Small Aromatic Molecules, Adv. Funct. Mater. 34 (2024) 2311578. https://doi.org/10.1002/adfm.202311578.
[39] C.L. Hapenciuc, M. Oane, A. Visan, C. Ristoscu, A. Stochioiu, I. Urzica, M. Dumitru, S. Anghel, T. Borca-Tasciuc, I.N. Mihailescu, Hot probe technique for thin films Seebeck coefficient measurement, Results Eng. (2024) 102789. https://doi.org/10.1016/j.rineng.2024.102789.
[40] T. Hong, C. Guo, B. Qin, X. Zhang, X. Gao, L.-D. Zhao, Realizing ultrahigh room-temperature seebeck coefficient and thermoelectric properties in SnTe-based alloys through carrier modulation and band convergence, Acta Mater. 261 (2023) 119412. https://doi.org/10.1016/j.actamat.2023.119412.
[41] M. Hase, D. Tanisawa, K. Kohashi, R. Kamemura, S. Miyake, M. Takashiri, Determination of Seebeck coefficient originating from phonon-drag effect using Si single crystals at different carrier densities, Sci. Rep. 13 (2023) 13463. https://doi.org/10.1038/s41598-023-40685-6.
[42] L. Su, H. Shi, S. Wang, D. Wang, B. Qin, Y. Wang, C. Chang, L.-D. Zhao, Enhancing Carrier Mobility and Seebeck Coefficient by Modifying Scattering Factor, Adv. Energy Mater. 13 (2023) 2300312. https://doi.org/10.1002/aenm.202300312.
[43] R. Xiong, S. Masoumi, A. Pakdel, An Automatic Apparatus for Simultaneous Measurement of Seebeck Coefficient and Electrical Resistivity, Energies 16 (2023) 6319. https://doi.org/10.3390/en16176319.
[44] M.T. Chughtai, The Incorporation of Thermocouples in Knitted Structures, Eng. Technol. Appl. Sci. Res. 13 (2023) 11593–11597. https://doi.org/10.48084/etasr.6183.
[45] E. Bilotti, O. Fenwick, B.C. Schroeder, M. Baxendale, P. Taroni-Junior, T. Degousée, Z. Liu, 6.14 Organic Thermoelectric Composites Materials, in: Compr. Compos. Mater. II, Elsevier, 2018: pp. 408–430. https://doi.org/10.1016/B978-0-12-803581-8.10024-4.
[46] V.D. Das, N. Soundararajan, Size and temperature effects on the Seebeck coefficient of thin bismuth films, Phys. Rev. B 35 (1987) 5990–5996. https://doi.org/10.1103/PhysRevB.35.5990.
[47] T. Goto, J.H. Li, T. Hirai, Y. Maeda, R. Kato, A. Maesono, Measurements of the seebeck coefficient of thermoelectric materials by an AC method, Int. J. Thermophys. 18 (1997) 569–577. https://doi.org/10.1007/BF02575185.

[48] A. Bellucci, M. Girolami, D.M. Trucchi, Thermionic and thermoelectric energy conversion, in: Ultra-High Temp. Therm. Energy Storage Transf. Convers., Elsevier, 2021: pp. 253–284. https://doi.org/10.1016/B978-0-12-819955-8.00010-7.
[49] A.V. Da Rosa, J.C. Ordóñez, Thermoelectricity, in: Fundam. Renew. Energy Process., Elsevier, 2022: pp. 187–247. https://doi.org/10.1016/B978-0-12-816036-7.00015-4.
[50] T.N. Trong, M.N. Duc, The speed control system of BLDC using PID controller with PWM modulation technique, Int. J. Adv. Appl. Sci. 2 (2015) 47-51.
[51] O.A. Marzouk, Detailed and simplified plasma models in combined-cycle magnetohydrodynamic power systems, Int. J. Adv. Appl. Sci. 10 (2023) 96–108. https://doi.org/10.21833/ijaas.2023.11.013.
[52] A.S. Alateeq, Enhancing voltage gain and switching efficiency in a non-isolated buck-boost converter through integrated switching inductor configuration, Int. J. Adv. Appl. Sci. 10 (2023) 67–71. https://doi.org/10.21833/ijaas.2023.11.009.
[53] F. Asadi, N. Abut, ITAE criterion based controller for buck converter, Int. J. Adv. Appl. Sci. 4 (2016) 15–22. https://doi.org/10.21833/ijaas.2017.01.003.
[54] F. Asadi, N. Abut, I. Kandilli, Joy of controller design: Controller design based on Kocaeli university's converter dynamics toolbox for MATLAB, Int. J. Adv. Appl. Sci. 4 (2017) 5–10. https://doi.org/10.21833/ijaas.2017.07.002.
[55] F. Asadi, N. Abut, U. Akca, Designing a PI controller for Cuk converter using converter dynamics toolbox for MATLAB, Int. J. Adv. Appl. Sci. 4 (2017) 175–180. https://doi.org/10.21833/ijaas.2017.06.025.
[56] F. Asadi, N. Abut, I. Kandilli, Dynamics and control of a novel buck-boost converter with low stresses on switches and diodes, Int. J. Adv. Appl. Sci. 4 (2017) 149–153. https://doi.org/10.21833/ijaas.2017.08.021.
[57] F. Asadi, N. Abut, U. Akca, Development of a power electronics converter dynamics toolbox for MATLAB, Int. J. Adv. Appl. Sci. 4 (2017) 56–62. https://doi.org/10.21833/ijaas.2017.06.008.
[58] K.K. Ali, H.F. Ismael, B.A. Mahmood, M.A. Yousif, MHD Casson fluid with heat transfer in a liquid film over unsteady stretching plate, Int. J. Adv. Appl. Sci. 4 (2016) 55–58. https://doi.org/10.21833/ijaas.2017.01.008.
[59] D. Luo, Y. Yan, Y. Li, R. Wang, S. Cheng, X. Yang, D. Ji, A hybrid transient CFD-thermoelectric numerical model for automobile thermoelectric generator systems, Appl. Energy 332 (2023) 120502. https://doi.org/10.1016/j.apenergy.2022.120502.
[60] Y. Zhao, M. Lu, Y. Li, Y. Wang, M. Ge, Numerical investigation of an exhaust thermoelectric generator with a perforated plate, Energy 263 (2023) 125776. https://doi.org/10.1016/j.energy.2022.125776.
[61] T. Widodo Besar Riyadi, M. Effendy, B. Radiant Utomo, A. Tri Wijayanta, Performance of a photovoltaic-thermoelectric generator panel in combination with various solar tracking systems, Appl. Therm. Eng. 235 (2023) 121336. https://doi.org/10.1016/j.applthermaleng.2023.121336.
[62] W.-H. Chen, Y.-K. Lin, D. Luo, L. Jin, A.T. Hoang, L.H. Saw, S. Nižetić, Effects of material doping on the performance of thermoelectric generator with/without equal segments, Appl. Energy 350 (2023) 121709. https://doi.org/10.1016/j.apenergy.2023.121709.
[63] D. Luo, Y. Yan, Y. Li, X. Yang, H. Chen, Exhaust channel optimization of the automobile thermoelectric generator to produce the highest net power, Energy 281 (2023) 128319. https://doi.org/10.1016/j.energy.2023.128319.
[64] Y. Zhao, G. Zhang, L. Wen, S. Wang, Y. Wang, Y. Li, M. Ge, Experimental study on thermoelectric characteristics of intermediate fluid thermoelectric generator, Appl. Energy 365 (2024) 123263. https://doi.org/10.1016/j.apenergy.2024.123263.
[65] D. Yuan, W. Jiang, A. Sha, J. Xiao, W. Wu, T. Wang, Technology method and functional characteristics of road thermoelectric generator system based on Seebeck effect, Appl. Energy 331 (2023) 120459. https://doi.org/10.1016/j.apenergy.2022.120459.
[66] M.N. Hanani, J. Sampe, J. Jaffar, N.H. Mohd Yunus, Development of a Hybrid Solar and Waste Heat Thermal Energy Harvesting System, Eng. Technol. Appl. Sci. Res. 13 (2023) 10680–10684. https://doi.org/10.48084/etasr.5561.
[67] C. Savescu, V. Petrescu, D. Comeaga, R. Carlanescu, M. Roman, D. Lale, A. Mitru, Thermal Potential of a Twin-Screw Compressor as Thermoelectric Energy Harvesting Source, Eng. Technol. Appl. Sci. Res. 14 (2024) 13449–13455. https://doi.org/10.48084/etasr.6417.
[68] EVERREDtronics, Thermoelectric Generator, (n.d.). https://www.everredtronics.com/thermoelectric.generator.html (accessed October 8, 2022).
[69] S. Pandit, R. Mal, A. Purwar, K. Kumari, Waste heat regeneration from thermoelectric generator based improved biomass cookstove (TIBC): Modelling of TEG system utilizing DC-DC converter with fuzzy logic MPPT, Energy Convers. Manag. 300 (2024) 117977. https://doi.org/10.1016/j.enconman.2023.117977.
[70] J. Faraj, W. Salameh, A.A. Takash, H.E. Hajj, C. Castelain, M. Mortazavi, R. Taher, M. Khaled, Boosting Diesel Generators Power with Thermoelectric Generators and Integrated Oil Tank – Thermal Modeling and Parametric Study, Int. J. Thermofluids (2024) 100632. https://doi.org/10.1016/j.ijft.2024.100632.
[71] J. Ider, F.Y. Assahi, A.F. Oliveira, R.M. Rubinger, C.P.L. Rubinger, Efficiency analysis of thermoelectric generators, Mater. Sci. Eng. B 300 (2024) 117122. https://doi.org/10.1016/j.mseb.2023.117122.
[72] Thermoelectric Generator, TEG10W stove top TEG Generator, (n.d.). https://thermoelectric-generator.com/product/teg10w-stove-top-teg-generator (accessed October 8, 2022).

[73] Thermoelectric Generator, IPOWER TOWER 10W Thermoelectric Generator 5V/1.2V-12V POWER Blue, (n.d.). https://thermoelectric-generator.com/product/ipower-tower-10w-thermoelectric-generator-5v1-2v-12v-power-blue (accessed October 8, 2022).

[74] C.E. Kinsella, S.M. O'Shaughnessy, M.J. Deasy, M. Duffy, A.J. Robinson, Battery charging considerations in small scale electricity generation from a thermoelectric module, Appl. Energy 114 (2014) 80–90. https://doi.org/10.1016/j.apenergy.2013.09.025.

[75] T. Kajikawa, Thermoelectric Application for Power Generation in Japan, in: 2010: pp. 83–92. https://doi.org/10.4028/www.scientific.net/AST.74.83.

[76] P.A.J. Stecanella, M.A.A. Faria, E.G. Domingues, P.H.G. Gomes, W.P. Calixto, A.J. Alves, Eletricity generation using thermoelectric generator - TEG, in: 2015 IEEE 15th Int. Conf. Environ. Electr. Eng. EEEIC, IEEE, Rome, Italy, 2015: pp. 2104–2108. https://doi.org/10.1109/EEEIC.2015.7165502.

[77] M. Singh, J. Singh, Anshula, P. Kuchroo, H. Bhatia, S. Bhagat, G. Sharma, E. Sidhu, Efficient autonomous solar panel and thermo-electric generator (TEG) integrated hybrid energy harvesting system, in: 2016 Prog. Electromagn. Res. Symp. PIERS, IEEE, Shanghai, China, 2016: pp. 1764–1768. https://doi.org/10.1109/PIERS.2016.7734785.

[78] D. Luo, R. Wang, W. Yu, W. Zhou, A novel optimization method for thermoelectric module used in waste heat recovery, Energy Convers. Manag. 209 (2020) 112645. https://doi.org/10.1016/j.enconman.2020.112645.

[79] Y. Jia, Z. Zhang, C. Wang, H. Sun, W. Zhang, Design and parameter study of a thermoelectric generator for waste heat recycling in flexible micro-light-emitting diodes, Appl. Therm. Eng. 200 (2022) 117568. https://doi.org/10.1016/j.applthermaleng.2021.117568.

[80] M.A. Zoui, S. Bentouba, D. Velauthapillai, N. Zioui, M. Bourouis, Design and characterization of a novel finned tubular thermoelectric generator for waste heat recovery, Energy 253 (2022) 124083. https://doi.org/10.1016/j.energy.2022.124083.

[81] J. Deng, F. Zhou, B. Shi, J.L. Torero, H. Qi, P. Liu, S. Ge, Z. Wang, C. Chen, Waste heat recovery, utilization and evaluation of coalfield fire applying heat pipe combined thermoelectric generator in Xinjiang, China, Energy 207 (2020) 118303. https://doi.org/10.1016/j.energy.2020.118303.

[82] S. Hooshmand Zaferani, M. Jafarian, D. Vashaee, R. Ghomashchi, Thermal Management Systems and Waste Heat Recycling by Thermoelectric Generators—An Overview, Energies 14 (2021) 5646. https://doi.org/10.3390/en14185646.

[83] Y. Peng, X. Zhang, J. Liu, S. Li, Y. Mou, J. Xu, M. Chen, Waste heat recycling of high-power lighting through chips on thermoelectric generator, Energy Convers. Manag. 243 (2021) 114329. https://doi.org/10.1016/j.enconman.2021.114329.

[84] M.R.A. BhuiYan, H. Mamur, M.A. Üstüner, Ö.F. DiLmaç, Current and Future Trend Opportunities of Thermoelectric Generator Applications in Waste Heat Recovery, Gazi Univ. J. Sci. 35 (2022) 896–915. https://doi.org/10.35378/gujs.934901.

[85] A.A. Sinha, K. Srivastava, A.S. Rajpoot, T. Choudhary, S.P. Pandey, Sanjay, A thermodynamic approach to analyze energy, exergy, emission, and sustainability (3E-S) performance by utilizing low temperature waste heat in SOFC–CHP-TEG system, Int. J. Hydrog. Energy 63 (2024) 1088–1104. https://doi.org/10.1016/j.ijhydene.2024.03.194.

[86] M. Alam, K. Kumar, V. Dutta, Dynamic modeling and experimental analysis of waste heat recovery from the proton exchange membrane fuel cell using thermoelectric generator, Therm. Sci. Eng. Prog. 19 (2020) 100627. https://doi.org/10.1016/j.tsep.2020.100627.

[87] M. Saufi Sulaiman, B. Singh, W.A.N.W. Mohamed, Experimental and theoretical study of thermoelectric generator waste heat recovery model for an ultra-low temperature PEM fuel cell powered vehicle, Energy 179 (2019) 628–646. https://doi.org/10.1016/j.energy.2019.05.022.

[88] M.A. Qasim, V.I. Velkin, S.E. Shcheklein, Experimental and Implementation of a 15 × 10 TEG Array of a Thermoelectric Power Generation System Using Two-Pass Flow of a Tap Water Pipeline Based on Renewable Energy, Appl. Sci. 12 (2022) 7948. https://doi.org/10.3390/app12157948.

[89] Z. Dashevsky, A. Jarashneli, Y. Unigovski, B. Dzunzda, F. Gao, R. Shneck, Development of a High Perfomance Gas Thermoelectric Generator (TEG) with Possibible Use of Waste Heat, Energies 15 (2022) 3960. https://doi.org/10.3390/en15113960.

[90] M. Gharzi, A.M. Kermani, H. Tash Shamsabadi, Experimental investigation of a parabolic trough collector-thermoelectric generator (PTC-TEG) hybrid solar system with a pressurized heat transfer fluid, Renew. Energy 202 (2023) 270–279. https://doi.org/10.1016/j.renene.2022.11.110.

[91] D. Ji, H. Cai, Z. Ye, D. Luo, G. Wu, A. Romagnoli, Comparison between thermoelectric generator and organic Rankine cycle for low to medium temperature heat source: A Techno-economic analysis, Sustain. Energy Technol. Assess. 55 (2023) 102914. https://doi.org/10.1016/j.seta.2022.102914.

[92] Z. Liu, K. Cheng, Z. Wang, Y. Wang, C. Ha, J. Qin, Performance analysis of the heat pipe-based thermoelectric generator (HP-TEG) energy system using in-situ resource for heat storage applied to the early-period lunar base, Appl. Therm. Eng. 218 (2023) 119303. https://doi.org/10.1016/j.applthermaleng.2022.119303.

[93] Y. Zhao, W. Li, X. Zhao, Y. Wang, D. Luo, Y. Li, M. Ge, Energy and exergy analysis of a thermoelectric generator system for automotive exhaust waste heat recovery, Appl. Therm. Eng. 239 (2024) 122180. https://doi.org/10.1016/j.applthermaleng.2023.122180.

[94] M. Naveed Gull, T. Ahmad Cheema, A. Imran, N. Uz Zaman, H. Ahmed Sher, C. Woo Park, Multiphysics performance evaluation of thermoelectric generator arrays, Appl. Therm. Eng. 249 (2024) 123348. https://doi.org/10.1016/j.applthermaleng.2024.123348.
[95] W. Zhang, J. Calderon-Sanchez, D. Duque, A. Souto-Iglesias, Computational Fluid Dynamics (CFD) applications in Floating Offshore Wind Turbine (FOWT) dynamics: A review, Appl. Ocean Res. 150 (2024) 104075. https://doi.org/10.1016/j.apor.2024.104075.
[96] M. Aichouni, L. Kolsi, N. Ait-Messaoudenne, W. Aich, Computational study of the performance of the Etoile flow conditioner, Int. J. Adv. Appl. Sci. 3 (2016) 25–30.
[97] O.A. Marzouk, A.H. Nayfeh, Characterization of the flow over a cylinder moving harmonically in the cross-flow direction, Int. J. Non-Linear Mech. 45 (2010) 821–833. https://doi.org/10.1016/j.ijnonlinmec.2010.06.004.
[98] K. Kiryanto, A.W.B. Santosa, S. Samuel, A. Firdhaus, Sea-keeping analysis of hospital catamarans for handling COVID-19 patients on remote islands with a numerical approach, Int. J. Adv. Appl. Sci. 9 (2022) 128–135. https://doi.org/10.21833/ijaas.2022.08.016.
[99] O.A. Marzouk, One-way and two-way couplings of CFD and structural models and application to the wake-body interaction, Appl. Math. Model. 35 (2011) 1036–1053. https://doi.org/10.1016/j.apm.2010.07.049.
[100] S. Serdarevic-Kadic, Wave drag coefficient of nonaxisymmetric irregular-shaped bodies, Int. J. Adv. Appl. Sci. 9 (2022) 98–107. https://doi.org/10.21833/ijaas.2022.12.013.
[101] O.A. Marzouk, Direct Numerical Simulations of the Flow Past a Cylinder Moving With Sinusoidal and Nonsinusoidal Profiles, J. Fluids Eng. 131 (2009) 121201. https://doi.org/10.1115/1.4000406.
[102] A. Catovic, E. Kljuno, Prediction of aerodynamic coefficients for irregularly shaped body using numerical simulations, Int. J. Adv. Appl. Sci. 5 (2018) 71–85. https://doi.org/10.21833/ijaas.2018.07.010.
[103] O.A. Marzouk, Characteristics of the Flow-Induced Vibration and Forces With 1- and 2-DOF Vibrations and Limiting Solid-to-Fluid Density Ratios, J. Vib. Acoust. 132 (2010) 041013. https://doi.org/10.1115/1.4001503.
[104] Q. Zong, X. Wu, A review of computational fluid dynamics (CFD) methodology and analysis on airflow and sand transport over aeolian landforms, CATENA 241 (2024) 108010. https://doi.org/10.1016/j.catena.2024.108010.
[105] O.A. Marzouk, The Sod gasdynamics problem as a tool for benchmarking face flux construction in the finite volume method, Sci. Afr. 10 (2020) e00573. https://doi.org/10.1016/j.sciaf.2020.e00573.
[106] P.C. Africa, I. Fumagalli, M. Bucelli, A. Zingaro, M. Fedele, L. Dede', A. Quarteroni, lifex-cfd: An open-source computational fluid dynamics solver for cardiovascular applications, Comput. Phys. Commun. 296 (2024) 109039. https://doi.org/10.1016/j.cpc.2023.109039.
[107] A. Bouziane, A. Alami, M. Zaitri, B. Bouchame, M. Bouchetara, Investigation of Swirl Stabilized CH4 Air Flame with Varied Hydrogen Content by using Computational Fluid Dynamics (CFD) to Study the Temperature Field and Flame Shape, Eng. Technol. Appl. Sci. Res. 11 (2021) 6943–6948. https://doi.org/10.48084/etasr.4034.
[108] O. Marzouk, A two-step computational aeroacoustics method applied to high-speed flows, Noise Control Eng. J. 56 (2008) 396. https://doi.org/10.3397/1.2978229.
[109] S. Tomescu, I.O. Bucur, Numerical Investigation of Oil Gas Separation with the Use of VOF CFD, Eng. Technol. Appl. Sci. Res. 11 (2021) 7841–7845. https://doi.org/10.48084/etasr.4446.
[110] A. Lipej, Challenges in the Numerical Analysis of Centrifugal Pumps: Energetic, Cavitation and Dynamic Characteristics, Eng. Technol. Appl. Sci. Res. 12 (2022) 8217–8222. https://doi.org/10.48084/etasr.4647.
[111] O.A. Marzouk, Flow control using bifrequency motion, Theor. Comput. Fluid Dyn. 25 (2011) 381–405. https://doi.org/10.1007/s00162-010-0206-6.
[112] M. Elashmawy, 3D-CFD Simulation of Confined Cross-Flow Injection Process Using Single Piston Pump, Eng. Technol. Appl. Sci. Res. 7 (2017) 2308–2312. https://doi.org/10.48084/etasr.1561.
[113] F.P. Lucas, R. Huebner, Numerical Simulation of Single-Phase and Two-Phase Flows in Separator Vessels with Inclined Half-Pipe Inlet Device Applied in Reciprocating Compressors, Eng. Technol. Appl. Sci. Res. 8 (2018) 2897–2900. https://doi.org/10.48084/etasr.1993.
[114] M.W. Khalid, M. Ahsan, Computational Fluid Dynamics Analysis of Compressible Flow Through a Converging-Diverging Nozzle using the k-ε Turbulence Model, Eng. Technol. Appl. Sci. Res. 10 (2020) 5180–5185. https://doi.org/10.48084/etasr.3140.
[115] O.A. Marzouk, Estimated electric conductivities of thermal plasma for air-fuel combustion and oxy-fuel combustion with potassium or cesium seeding, Heliyon 10 (2024) e31697. https://doi.org/10.1016/j.heliyon.2024.e31697.
[116] W.F. Lima, R. Huebner, Optimization of Air Distribution in a Baghouse Filter Using Computational Fluid Dynamics, Eng. Technol. Appl. Sci. Res. 9 (2019) 4452–4456. https://doi.org/10.48084/etasr.2732.
[117] O.A. Marzouk, Temperature-Dependent Functions of the Electron–Neutral Momentum Transfer Collision Cross Sections of Selected Combustion Plasma Species, Appl. Sci. 13 (2023) 11282. https://doi.org/10.3390/app132011282.
[118] V. Dragan, A Numerical Proof of Concept for Thermal Flow Control, Eng. Technol. Appl. Sci. Res. 7 (2017) 1387–1390. https://doi.org/10.48084/etasr.974.
[119] O.A. Marzouk, Contrasting the Cartesian and polar forms of the shedding-induced force vector in response to 12 subharmonic and superharmonic mechanical excitations, Fluid Dyn. Res. 42 (2010) 035507. https://doi.org/10.1088/0169-5983/42/3/035507.

[120] A. Sarosh, A. Hussain, E. Pervaiz, M. Ahsan, Computational Fluid Dynamics (CFD) Analysis of Phthalic Anhydride's Yield Using Lab Synthesized and Commercially Available (V2O5/TiO2) Catalyst, Eng. Technol. Appl. Sci. Res. 8 (2018) 2821–2826. https://doi.org/10.48084/etasr.1954.
[121] O.A. Marzouk, A.H. Nayfeh, Reduction of the loads on a cylinder undergoing harmonic in-line motion, Phys. Fluids 21 (2009) 083103. https://doi.org/10.1063/1.3210774.
[122] V. Dragan, I. Malael, B. Gherman, A Comparative Analysis Between Optimized and Baseline High Pressure Compressor Stages Using Tridimensional Computational Fluid Dynamics, Eng. Technol. Appl. Sci. Res. 6 (2016) 1103–1108. https://doi.org/10.48084/etasr.696.
[123] COMSOL, COMSOL Multiphysics® Software - Understand, Predict, and Optimize, (2024). https://www.comsol.com/comsol-multiphysics (accessed June 14, 2024).
[124] J.A. Gomez-Sanchez, L. De Souza Ribero Bueno, P. Bertemes-Filho, Evaluation of electric field in polymeric electrodes geometries for liquid biosensing applications using COMSOL multiphysics, Sens. Bio-Sens. Res. 44 (2024) 100663. https://doi.org/10.1016/j.sbsr.2024.100663.
[125] Y. Wang, J. Chen, D. Li, L. Shi, H. Chi, Y. Ma, Simulation of S transport equation for hexagonal-z reactor using the COMSOL Multiphysics software, Nucl. Eng. Des. 416 (2024) 112746. https://doi.org/10.1016/j.nucengdes.2023.112746.
[126] C. Zhang, P. Duan, Y. Cheng, N. Chen, H. Huang, F. Xiong, S. Dong, A 2D stability analysis of the rock surrounding underground liquified natural gas storage cavern based on COMSOL Multiphysics, Energy Geosci. 5 (2024) 100301. https://doi.org/10.1016/j.engeos.2024.100301.
[127] B. Sezgin, D.G. Caglayan, Y. Devrim, T. Steenberg, I. Eroglu, Modeling and sensitivity analysis of high temperature PEM fuel cells by using Comsol Multiphysics, Int. J. Hydrog. Energy 41 (2016) 10001–10009. https://doi.org/10.1016/j.ijhydene.2016.03.142.
[128] D. Salvi, D. Boldor, G.M. Aita, C.M. Sabliov, COMSOL Multiphysics model for continuous flow microwave heating of liquids, J. Food Eng. 104 (2011) 422–429. https://doi.org/10.1016/j.jfoodeng.2011.01.005.
[129] M. Vajdi, F. Sadegh Moghanlou, F. Sharifianjazi, M. Shahedi Asl, M. Shokouhimehr, A review on the Comsol Multiphysics studies of heat transfer in advanced ceramics, J. Compos. Compd. 2 (2020) 35–44. https://doi.org/10.29252/jcc.2.1.5.
[130] Y. Genc, E. Altınağaç, L. Trabzon, Experimental validation for Comsol model of a DEP device, Int. J. Adv. Appl. Sci. 2 (2015) 42–46.
[131] S. Moorat, A.A. Ursani, A. Memon, N.F.M. Nasir, M. Nour, Transdermal drug delivery using low-frequency sonophoresis: COMSOL simulation of piezoelectric array transducers, Int. J. Adv. Appl. Sci. 11 (2024) 59–67. https://doi.org/10.21833/ijaas.2024.06.007.
[132] S. Lucarini, E. Martínez-Pañeda, UMAT4COMSOL: An Abaqus user material (UMAT) subroutine wrapper for COMSOL, Adv. Eng. Softw. 190 (2024) 103610. https://doi.org/10.1016/j.advengsoft.2024.103610.
[133] D. Champier, Thermoelectric generators: A review of applications, Energy Convers. Manag. 140 (2017) 167–181. https://doi.org/10.1016/j.enconman.2017.02.070.
[134] R.N.A.R.A. Shah, F.L.M. Redzuan, S.A. Zaki, A.F. Mohammad, F. Yakub, A Review on Thermoelectric Generators: Structural Optimization and Economic Analysis, J. Adv. Res. Fluid Mech. Therm. Sci. 105 (2023) 99–114. https://doi.org/10.37934/arfmts.105.2.99114.
[135] J. Asadi, P. Kazempoor, Advancing power plant decarbonization with a flexible hybrid carbon capture system, Energy Convers. Manag. 299 (2024) 117821. https://doi.org/10.1016/j.enconman.2023.117821.
[136] P. Liang, Y. Guo, T.U.K. Nutakki, M.K. Agrawal, T. Muhammad, S.F. Ahmad, A.Y.A. Bani Ahmad, M. Qin, Comprehensive assessment and sustainability improvement of a natural gas power plant utilizing an environmentally friendly combined cooling heating and power-desalination arrangement, J. Clean. Prod. 436 (2024) 140387. https://doi.org/10.1016/j.jclepro.2023.140387.
[137] S. Upasana, S. Avtar, Reliability analysis of CPP system where the working of standby unit depends on connecting unit, Int. J. Adv. Appl. Sci. 9 (2022) 72–78. https://doi.org/10.21833/ijaas.2022.08.009.
[138] M. Masmali, M.I. Elimy, M. Fterich, E. Touti, G. Abbas, Comparative Studies on Load Frequency Control with Different Governors connected to Mini Hydro Power Plant via PSCAD Software, Eng. Technol. Appl. Sci. Res. 14 (2024) 12975–12983. https://doi.org/10.48084/etasr.6722.
[139] N.T.A. Truong, N.B. Khanh, L.N. Giap, B.T. Trung, N.P. Le, T.T. Vinh, Feasibility Analysis of Wind Power Plant in South East Region, Vietnam, Eng. Technol. Appl. Sci. Res. 14 (2024) 15779–15783. https://doi.org/10.48084/etasr.7849.
[140] M.O. Karkush, Impacts of Soil Contamination on the Response of Piles Foundation under a Combination of Loading, Eng. Technol. Appl. Sci. Res. 6 (2016) 917–922. https://doi.org/10.48084/etasr.616.
[141] Z.A. Shahani, A.A. Hashmani, M.M. Shaikh, Steady State Stability Analysis and Improvement using Eigenvalues and PSS: A Case Study of a Thermal Power Plant in Jamshoro, Pakistan, Eng. Technol. Appl. Sci. Res. 10 (2020) 5301–5306. https://doi.org/10.48084/etasr.3318.
[142] A. Mursadin, A.Y. Iriyanto, Modeling and Predicting Steam Power Plant Condenser Vacuum based on Small-sized Operation Data, Eng. Technol. Appl. Sci. Res. 14 (2024) 15233–15238. https://doi.org/10.48084/etasr.7574.

[143] M.R.S. Malik, V.S. Priya, ANN-weighted Distance Grey Wolf Optimizer for NOx Emission Optimization in Coal Fired Boilers of a Thermal Power Plant, Eng. Technol. Appl. Sci. Res. 14 (2024) 15361–15366. https://doi.org/10.48084/etasr.7847.
[144] A. Lachheb, R. Marouani, C. Mahamat, S. Skouri, S. Bouadila, Fostering Sustainability through the Integration of Renewable Energy in an Agricultural Hydroponic Greenhouse, Eng. Technol. Appl. Sci. Res. 14 (2024) 13398–13407. https://doi.org/10.48084/etasr.6939.
[145] T. Eldamaty, A.G. Ahmed, M.M. Helal, GIS-Based Multi Criteria Analysis for Solar Power Plant Site Selection Support in Mecca, Eng. Technol. Appl. Sci. Res. 13 (2023) 10963–10968. https://doi.org/10.48084/etasr.5927.
[146] Y. Kassem, H. Camur, O.A.M. Abughinda, Solar Energy Potential and Feasibility Study of a 10MW Grid-connected Solar Plant in Libya, Eng. Technol. Appl. Sci. Res. 10 (2020) 5358–5366. https://doi.org/10.48084/etasr.3607.
[147] H. Mamur, Ö.F. Dilmaç, J. Begum, M.R.A. Bhuiyan, Thermoelectric generators act as renewable energy sources, Clean. Mater. 2 (2021) 100030. https://doi.org/10.1016/j.clema.2021.100030.
[148] Y. He, X. Chen, Y. Zheng, G. Chen, Numerical simulation of a wire–plate solid-state fan for ultra-quiet museum display cases, Indoor Built Environ. 29 (2020) 1028–1037. https://doi.org/10.1177/1420326X19876100.
[149] A. Rajagopalan, B. Guerke, J.J.-M. Yang, Early Detection of Failure in Solid State Devices Using 4 Corner Targeted Testing, in: 2024 Annu. Reliab. Maintainab. Symp. RAMS, IEEE, Albuquerque, NM, USA, 2024: pp. 1–5. https://doi.org/10.1109/RAMS51492.2024.10457788.
[150] M. Zebarjadi, Power Generation Using Solid-State Heat Engines, in: P.M. Norris, L.E. Friedersdorf (Eds.), Women Nanotechnol., Springer International Publishing, Cham, 2020: pp. 71–83. https://doi.org/10.1007/978-3-030-19951-7_6.
[151] N.I. Gross, P. Svasta, Evaluation of Usage of Solid State MOSFET Switches in Test Equipment for PSI5 Automotive Sensors, in: 2023 IEEE 29th Int. Symp. Des. Technol. Electron. Packag. SIITME, IEEE, Craiova, Romania, 2023: pp. 189–193. https://doi.org/10.1109/SIITME59799.2023.10431244.
[152] F. Najmi, J. He, L. Cremaschi, Z.-Y. Cheng, Electrocaloric devices part II: All-solid heat pump without moving parts, J. Adv. Dielectr. 10 (2020) 2050029. https://doi.org/10.1142/S2010135X20500290.
[153] J. Morris, K. Sander, J. MacDonald, A Blueprint for Solid State Automatic Bus Transfer Switches, Nav. Eng. J. 112 (2000) 59–67. https://doi.org/10.1111/j.1559-3584.2000.tb03381.x.
[154] N. Vázquez, J. Vaquero, Inverters, in: Power Electron. Handb., Elsevier, 2024: pp. 293–343. https://doi.org/10.1016/B978-0-323-99216-9.00001-9.
[155] J.M. Pearce, R. Parncutt, Quantifying Global Greenhouse Gas Emissions in Human Deaths to Guide Energy Policy, Energies 16 (2023) 6074. https://doi.org/10.3390/en16166074.
[156] J.M.-F. Johnson, A.J. Franzluebbers, S.L. Weyers, D.C. Reicosky, Agricultural opportunities to mitigate greenhouse gas emissions, Environ. Pollut. 150 (2007) 107–124. https://doi.org/10.1016/j.envpol.2007.06.030.
[157] O.A. Marzouk, Zero Carbon Ready Metrics for a Single-Family Home in the Sultanate of Oman Based on EDGE Certification System for Green Buildings, Sustainability 15 (2023) 13856. https://doi.org/10.3390/su151813856.
[158] R. Rath, P. Kumar, S. Mohanty, S.K. Nayak, Recent advances, unsolved deficiencies, and future perspectives of hydrogen fuel cells in transportation and portable sectors, Int. J. Energy Res. 43 (2019) 8931–8955. https://doi.org/10.1002/er.4795.
[159] Y. Gong, J. Liu, Udabala, Y. Su, Y. Li, Q. Zhao, J. Liu, R. Huang, Transaction Analysis of Self-owned Power Plant Participation in Renewable Energy Consumption, in: 2023 2nd Asian Conf. Front. Power Energy ACFPE, 2023: pp. 277–281. https://doi.org/10.1109/ACFPE59335.2023.10455203.
[160] O.A. Marzouk, Radiant Heat Transfer in Nitrogen-Free Combustion Environments, Int. J. Nonlinear Sci. Numer. Simul. 19 (2018) 175–188. https://doi.org/10.1515/ijnsns-2017-0106.
[161] J. Hansen, M. Sato, Greenhouse gas growth rates, Proc. Natl. Acad. Sci. 101 (2004) 16109–16114. https://doi.org/10.1073/pnas.0406982101.
[162] R.C. Hyman, J.M. Reilly, M.H. Babiker, A. De Masin, H.D. Jacoby, Modeling non-CO_2 Greenhouse Gas Abatement, Environ. Model. Assess. 8 (2003) 175–186. https://doi.org/10.1023/A:1025576926029.
[163] O.A. Marzouk, Expectations for the Role of Hydrogen and Its Derivatives in Different Sectors through Analysis of the Four Energy Scenarios: IEA-STEPS, IEA-NZE, IRENA-PES, and IRENA-1.5°C, Energies 17 (2024) 646. https://doi.org/10.3390/en17030646.
[164] O.A. Marzouk, Adiabatic Flame Temperatures for Oxy-Methane, Oxy-Hydrogen, Air-Methane, and Air-Hydrogen Stoichiometric Combustion using the NASA CEARUN Tool, GRI-Mech 3.0 Reaction Mechanism, and Cantera Python Package, Eng. Technol. Appl. Sci. Res. 13 (2023) 11437–11444. https://doi.org/10.48084/etasr.6132.
[165] J. Lelieveld, K. Klingmüller, A. Pozzer, R.T. Burnett, A. Haines, V. Ramanathan, Effects of fossil fuel and total anthropogenic emission removal on public health and climate, Proc. Natl. Acad. Sci. 116 (2019) 7192–7197. https://doi.org/10.1073/pnas.1819989116.
[166] M.Z. Jacobson, Short-term effects of controlling fossil-fuel soot, biofuel soot and gases, and methane on climate, Arctic ice, and air pollution health, J. Geophys. Res. Atmospheres 115 (2010) 2009JD013795. https://doi.org/10.1029/2009JD013795.

[167] K. Mukhopadhyay, O. Forssell, An empirical investigation of air pollution from fossil fuel combustion and its impact on health in India during 1973–1974 to 1996–1997, Ecol. Econ. 55 (2005) 235–250. https://doi.org/10.1016/j.ecolecon.2004.09.022.
[168] F.P. Perera, Multiple Threats to Child Health from Fossil Fuel Combustion: Impacts of Air Pollution and Climate Change, Environ. Health Perspect. 125 (2017) 141–148. https://doi.org/10.1289/EHP299.
[169] F. Perera, Pollution from Fossil-Fuel Combustion is the Leading Environmental Threat to Global Pediatric Health and Equity: Solutions Exist, Int. J. Environ. Res. Public. Health 15 (2018) 16. https://doi.org/10.3390/ijerph15010016.
[170] B.D. Fath, S.E. Jørgensen, M. Cole, eds., Managing Air Quality and Energy Systems, 2nd ed., CRC Press, Second edition. | Boca Raton : CRC Press, 2020. | Series: Applied ecology and environmental management, 2020. https://doi.org/10.1201/9781003043461.
[171] P. Smith, D. Martino, Z. Cai, D. Gwary, H. Janzen, P. Kumar, B. McCarl, S. Ogle, F. O'Mara, C. Rice, B. Scholes, O. Sirotenko, M. Howden, T. McAllister, G. Pan, V. Romanenkov, U. Schneider, S. Towprayoon, M. Wattenbach, J. Smith, Greenhouse gas mitigation in agriculture, Philos. Trans. R. Soc. B Biol. Sci. 363 (2007) 789–813. https://doi.org/10.1098/rstb.2007.2184.
[172] B. Patnaik, S.C. Swain, U.K. Rout, An Experimental Study of Greenhouse Gas Concentration on the Maximum Power Point of Solar PV Panels, Eng. Technol. Appl. Sci. Res. 10 (2020) 6200–6203. https://doi.org/10.48084/etasr.3682.
[173] H. Jouhara, A. Żabnieńska-Góra, N. Khordehgah, Q. Doraghi, L. Ahmad, L. Norman, B. Axcell, L. Wrobel, S. Dai, Thermoelectric generator (TEG) technologies and applications, Int. J. Thermofluids 9 (2021) 100063. https://doi.org/10.1016/j.ijft.2021.100063.
[174] O.A. Marzouk, Land-Use competitiveness of photovoltaic and concentrated solar power technologies near the Tropic of Cancer, Sol. Energy 243 (2022) 103–119. https://doi.org/10.1016/j.solener.2022.07.051.
[175] O.A. Marzouk, Energy Generation Intensity (EGI) of Solar Updraft Tower (SUT) Power Plants Relative to CSP Plants and PV Power Plants Using the New Energy Simulator "Aladdin," Energies 17 (2024) 405. https://doi.org/10.3390/en17020405.
[176] O.A. Marzouk, Lookup Tables for Power Generation Performance of Photovoltaic Systems Covering 40 Geographic Locations (Wilayats) in the Sultanate of Oman, with and without Solar Tracking, and General Perspectives about Solar Irradiation, Sustainability 13 (2021) 13209. https://doi.org/10.3390/su132313209.
[177] J.L. Cox, W.T. Hamilton, A.M. Newman, Parametric analysis on optimized design of hybrid solar power plants, Sol. Energy 252 (2023) 195–217. https://doi.org/10.1016/j.solener.2023.01.016.
[178] M. Saha, O. Tregenza, J. Twelftree, C. Hulston, A review of thermoelectric generators for waste heat recovery in marine applications, Sustain. Energy Technol. Assess. 59 (2023) 103394. https://doi.org/10.1016/j.seta.2023.103394.
[179] E. Garofalo, M. Bevione, L. Cecchini, F. Mattiussi, A. Chiolerio, Waste Heat to Power: Technologies, Current Applications, and Future Potential, Energy Technol. 8 (2020) 2000413. https://doi.org/10.1002/ente.202000413.
[180] O.A. Marzouk, Performance analysis of shell-and-tube dehydrogenation module: Dehydrogenation module, Int. J. Energy Res. 41 (2017) 604–610. https://doi.org/10.1002/er.3637.
[181] O.A. Marzouk, Compilation of Smart Cities Attributes and Quantitative Identification of Mismatch in Rankings, J. Eng. 2022 (2022) 1–13. https://doi.org/10.1155/2022/5981551.
[182] O.A. Marzouk, Urban air mobility and flying cars: Overview, examples, prospects, drawbacks, and solutions, Open Eng. 12 (2022) 662–679. https://doi.org/10.1515/eng-2022-0379.
[183] O.A. Marzouk, Subcritical and supercritical Rankine steam cycles, under elevated temperatures up to 900°C and absolute pressures up to 400 bara, Adv. Mech. Eng. 16 (2024) 1–18. https://doi.org/10.1177/16878132231221065.
[184] Tecteg Power Generator, TEG1-24111-6.0, (n.d.). https://tecteg.com/product/teg1-24111-6-0-2 (accessed October 18, 2023).
[185] Á. Fernández-Solas, L. Micheli, F. Almonacid, E.F. Fernández, Optical degradation impact on the spectral performance of photovoltaic technology, Renew. Sustain. Energy Rev. 141 (2021) 110782. https://doi.org/10.1016/j.rser.2021.110782.
[186] R. Daxini, Y. Wu, Review of methods to account for the solar spectral influence on photovoltaic device performance, Energy 286 (2024) 129461. https://doi.org/10.1016/j.energy.2023.129461.
[187] D. Cabral, G. Kosmadakis, E. Mathioulakis, Parametric comparison of a CPVT performance evaluation under standard testing procedures - ISO 9806:2017 and IEC 62108:2016 - for an automated and manual 2-axis tracking solar system stand, Energy Rep. 11 (2024) 1242–1255. https://doi.org/10.1016/j.egyr.2023.12.069.
[188] E.S. De Moura, H.S.A. Marques, D.B. Riffel, Assessment of photovoltaic I–V curve translation methods in real-world situations, Sol. Energy 276 (2024) 112654. https://doi.org/10.1016/j.solener.2024.112654.
[189] M. Steiner, G. Siefer, Translation of outdoor tandem PV module I–V measurements to a STC power rating, Prog. Photovolt. Res. Appl. 31 (2023) 862–869. https://doi.org/10.1002/pip.3691.
[190] İ. Kayri, An experimental study on optimization of coolant mass flow rate in a photovoltaic/thermal system, Proc. Inst. Mech. Eng. Part C J. Mech. Eng. Sci. 238 (2024) 1760–1777. https://doi.org/10.1177/09544062231212743.
[191] A. Almuwailhi, O. Zeitoun, Investigating the cooling of solar photovoltaic modules under the conditions of Riyadh, J. King Saud Univ. - Eng. Sci. 35 (2023) 123–136. https://doi.org/10.1016/j.jksues.2021.03.007.
[192] E. Moshksar, An Explicit and Accurate I-V Characteristic for Photovoltaic Modules Based on Piecewise Quadratic Function, Int. J. Ind. Electron. Control Optim. (2024). https://doi.org/10.22111/ieco.2024.48517.1554.

[193] J. Aulich, D. Chojniak, A.J. Bett, M. Steiner, F. Schindler, G. Siefer, M.C. Schubert, J.C. Goldschmidt, S.W. Glunz, Spectrometric Characterization for Triple-Junction Solar Cells, Sol. RRL 8 (2024) 2300783. https://doi.org/10.1002/solr.202300783.

[194] S. Cho, H. Song, P. Pandey, S.C. Cho, S. Yoon, W.H. Jeong, H. Ahn, S. Lee, J.-Y. Lee, Q. Shen, S.U. Lee, H. Choi, D.-W. Kang, Carboxylate Pseudo-Halide-Assisted crystallization and antioxidant strategy for stable wide bandgap tin perovskite photovoltaics, Chem. Eng. J. 497 (2024) 154720. https://doi.org/10.1016/j.cej.2024.154720.

[195] D. Liang, Z. Liang, R. Zhang, H. Yuan, X. Peng, Z. Yang, X. Wang, Y. Wang, Metamaterial absorber with broadband and superior absorption realized by optical nanotrapping hybrid cavity, Opt. Laser Technol. 177 (2024) 111007. https://doi.org/10.1016/j.optlastec.2024.111007.

[196] H. Zhang, S. Zhang, X. Ji, J. He, H. Guo, S. Wang, W. Wu, W.-H. Zhu, Y. Wu, Formamidinium Lead Iodide-Based Inverted Perovskite Solar Cells with Efficiency over 25 % Enabled by An Amphiphilic Molecular Hole-Transporter, Angew. Chem. 136 (2024) e202401260. https://doi.org/10.1002/ange.202401260.

[197] M. Ali, T. Maiyalagan, K.H. Lee, I. Choi, M.J. Ko, Utilizing molecular states of carbon quantum dots (CQDs) to efficiently harvest outdoor and indoor energy via luminescent solar concentrator, Surf. Interfaces 52 (2024) 104953. https://doi.org/10.1016/j.surfin.2024.104953.

[198] Y. Zheng, Z. Wang, Z. Yi, S. Cheng, C. Ma, B. Tang, T. Sun, S. Yu, G. Li, S. Ahmad, A wide-band solar absorber based on tungsten nano-strip resonator group and graphene for near-ultraviolet to near-infrared region, Diam. Relat. Mater. 142 (2024) 110843. https://doi.org/10.1016/j.diamond.2024.110843.

[199] Y. Zhang, G. Chen, Multifunctional photon conversion materials for enhancing silicon solar cells, Light Sci. Appl. 13 (2024) 87. https://doi.org/10.1038/s41377-024-01431-3.

[200] A.P. Kirk, Comment on CdTe solar cell efficiency, J. Alloys Metall. Syst. 5 (2024) 100050. https://doi.org/10.1016/j.jalmes.2023.100050.

[201] A.P. Kirk, Comment on 1.077 eV bandgap perovskite solar cell, Opt. Commun. 569 (2024) 130743. https://doi.org/10.1016/j.optcom.2024.130743.

[202] Y.R. Golive, A. Kottantharayil, J. Vasi, N. Shiradkar, Determining the optimal standard test condition correction procedure for high-throughput field I–V measurements of photovoltaic modules, Prog. Photovolt. Res. Appl. 30 (2022) 13–26. https://doi.org/10.1002/pip.3457.

[203] Y.R. Golive, A. Kottantharayil, N. Shiradkar, Sensitivity of accuracy of various standard test condition correction procedures to the errors in temperature coefficients of c-Si PV modules, Prog. Photovolt. Res. Appl. 30 (2022) 1087–1100. https://doi.org/10.1002/pip.3559.

[204] T. Takashima, Behavior of Interconnect-Failed PV Modules Under Standard Test Conditions and Actual Operation Conditions, IEEE J. Photovolt. 8 (2018) 1761–1766. https://doi.org/10.1109/JPHOTOV.2018.2868017.

[205] A.R. Toscano, J.C. Ortiz, N.D.A. Calderón, Technical analysis and evaluation of the energy performance of solar-activated absorption refrigeration systems: Case of the Caribbean Coast of Colombia, Procedia Comput. Sci. 231 (2024) 471–477. https://doi.org/10.1016/j.procs.2023.12.236.

[206] J. Liu, C. Li, P. Jia, J. Hao, L. Gao, J. Wang, L. Jiang, Large-Scale, Vertically Aligned 2D Subnanochannel Arrays by a Smectic Liquid Crystal Network for High-Performance Osmotic Energy Conversion, Adv. Mater. (2024) 2313695. https://doi.org/10.1002/adma.202313695.

[207] F.A. Pramadya, K.N. Kim, Promoting residential rooftop solar photovoltaics in Indonesia: Net-metering or installation incentives?, Renew. Energy 222 (2024) 119901. https://doi.org/10.1016/j.renene.2023.119901.

[208] L. Bardwell, A. Rahbari, Y. Wang, M. Amidy, J.D. Pye, Piggery waste to sustainable fuels via indirect supercritical water gasification and membrane reforming at 600°C: a techno-economic assessment, Sustain. Energy Fuels (2024) 10.1039.D3SE01634J. https://doi.org/10.1039/D3SE01634J.

[209] Thermal Electronics Corporation (TEC), Specification of Thermoelectric Module TEG1-24111-6.0, (n.d.). https://tecteg.com/wp-content/uploads/2016/08/TEG1-24111-6.0-Spec-sheet-.pdf (accessed February 20, 2023).

[210] A. Attar, H. Lee, G.J. Snyder, Optimum load resistance for a thermoelectric generator system, Energy Convers. Manag. 226 (2020) 113490. https://doi.org/10.1016/j.enconman.2020.113490.

[211] Ruchika, P. Gupta, D.K. Jain, R.S. Bhatia, Islanding detection technique for a distributed generation with perfectly matched load condition, in: 2017 Int. Conf. Comput. Commun. Autom. ICCCA, 2017: pp. 1503–1506. https://doi.org/10.1109/CCAA.2017.8230038.

[212] O.A. Marzouk, Evolutionary Computing Applied to Design Optimization, in: Vol. 2 27th Comput. Inf. Eng. Conf. Parts B, ASMEDC, Las Vegas, Nevada, USA, 2007: pp. 995–1003. https://doi.org/10.1115/DETC2007-35502.

[213] O.V. Varlamov, A. Grebennikov, Experimental Studies of Envelope Elimination and Restoration HF Power Amplifier Characteristics with Narrow-band Matched Load, in: 2022 Syst. Signal Synchronization Gener. Process. Telecommun. SYNCHROINFO, 2022: pp. 1–4. https://doi.org/10.1109/SYNCHROINFO55067.2022.9840873.

[214] K. Staszek, Six-Port Calibration Utilizing Matched Load and Unknown Calibration Loads, IEEE Trans. Microw. Theory Tech. 66 (2018) 4617–4626. https://doi.org/10.1109/TMTT.2018.2854725.

[215] Y. Shi, Z. Zhu, Y. Deng, W. Zhu, X. Chen, Y. Zhao, A real-sized three-dimensional numerical model of thermoelectric generators at a given thermal input and matched load resistance, Energy Convers. Manag. 101 (2015) 713–720. https://doi.org/10.1016/j.enconman.2015.06.020.

[216] K. Song, M. Bonnin, Nonlinear Stochastic Dynamics of an Energy Harvester with Matched Load, in: X. Rui, C. Liu (Eds.), Proc. 2nd Int. Conf. Mech. Syst. Dyn., Springer Nature, Singapore, 2024: pp. 4507–4519. https://doi.org/10.1007/978-981-99-8048-2_311.
[217] A. Kimuya, THE MODIFIED OHM'S LAW AND ITS IMPLICATIONS FOR ELECTRICAL CIRCUIT ANALYSIS, Eurasian J. Sci. Eng. Technol. 4 (2023) 59–70. https://doi.org/10.55696/ejset.1373552.
[218] T. Saxena, D.C.Y. Chek, M.L.P. Tan, V.K. Arora, Microcircuit Modeling and Simulation Beyond Ohm's Law, IEEE Trans. Educ. 54 (2011) 34–40. https://doi.org/10.1109/TE.2010.2041932.
[219] I. Bâldea, Y. Chen, M. Zhang, N. Xin, Y. Feng, J. Feng, C. Jia, X. Guo, Z. Xie, Breakdown of Ohm's Law in Molecular Junctions with Electrodes of Single-Layer Graphene, J. Phys. Chem. Lett. 15 (2024) 3267–3275. https://doi.org/10.1021/acs.jpclett.4c00387.
[220] T.L. Skvarenina, ed., The Power Electronics Handbook, 0 ed., CRC Press, 2018. https://doi.org/10.1201/9781420037067.
[221] S. Monk, Electronics Cookbook: Practical Electronic Recipes with Arduino and Raspberry Pi, First edition, O'Reilly, Sebastopol, CA, 2017.
[222] M. Flimel, D. Duplakova, E. Sukic, Implementation of Heat Flux Measuring Methods for Heat Transfer Coefficient Determination of In Situ Construction, Processes 9 (2021) 1970. https://doi.org/10.3390/pr9111970.
[223] M.M. Yasin, The theory and practice of benchmarking: then and now, Benchmarking Int. J. 9 (2002) 217–243. https://doi.org/10.1108/14635770210428992.
[224] O. Marzouk, Benchmarks for the Omani higher education students-faculty ratio (SFR) based on World Bank data, QS rankings, and THE rankings, Cogent Educ. 11 (2024) 2317117. https://doi.org/10.1080/2331186X.2024.2317117.
[225] J.P. Moriarty, A theory of benchmarking, Benchmarking Int. J. 18 (2011) 588–611. https://doi.org/10.1108/14635771111147650.
[226] V.-H. Le, H.-S. Do, V.-N. Phan, T.-H. Te, TQU-SLAM Benchmark Feature-based Dataset for Building Monocular VO, Eng. Technol. Appl. Sci. Res. 14 (2024) 15330–15337. https://doi.org/10.48084/etasr.7611.
[227] M. Morey, N. Gupta, M.M. Garg, A. Kumar, A comprehensive review of grid-connected solar photovoltaic system: Architecture, control, and ancillary services, Renew. Energy Focus 45 (2023) 307–330. https://doi.org/10.1016/j.ref.2023.04.009.
[228] P. Bórawski, L. Holden, A. Bełdycka-Bórawska, Perspectives of photovoltaic energy market development in the european union, Energy 270 (2023) 126804. https://doi.org/10.1016/j.energy.2023.126804.
[229] S. Li, T. Ma, D. Wang, Photovoltaic pavement and solar road: A review and perspectives, Sustain. Energy Technol. Assess. 55 (2023) 102933. https://doi.org/10.1016/j.seta.2022.102933.
[230] S. Al Ahmadi, Performances evaluation of a photovoltaic energy system for lighting storage, Int. J. Adv. Appl. Sci. 7 (2020) 28–33. https://doi.org/10.21833/ijaas.2020.08.004.
[231] I. Khenissi, N. Alkhateeb, R. Sellami, G.A. Alshammari, N.A. Alshammari, T. Guesmi, R. Neji, A soft computing technique based on PSO algorithm and energy management strategy for optimal allocation and placement of PVDG-BES units, Int. J. Adv. Appl. Sci. 10 (2023) 40–50. https://doi.org/10.21833/ijaas.2023.08.005.
[232] H. Hussein, A. Aloui, B. AlShammari, ANFIS-based PI controller for maximum power point tracking in PV systems, Int. J. Adv. Appl. Sci. 5 (2018) 90–96. https://doi.org/10.21833/ijaas.2018.02.015.
[233] H. Jerbi, Design and performance analysis of a PV solar powered water pumping system, Int. J. Adv. Appl. Sci. 4 (2017) 127–132. https://doi.org/10.21833/ijaas.2017.05.022.
[234] O.A. Marzouk, Tilt sensitivity for a scalable one-hectare photovoltaic power plant composed of parallel racks in Muscat, Cogent Eng. 9 (2022) 2029243. https://doi.org/10.1080/23311916.2022.2029243.
[235] B. Hallam, M. Kim, Y. Zhang, L. Wang, A. Lennon, P. Verlinden, P.P. Altermatt, P.R. Dias, The silver learning curve for photovoltaics and projected silver demand for net-zero emissions by 2050, Prog. Photovolt. Res. Appl. 31 (2023) 598–606. https://doi.org/10.1002/pip.3661.
[236] Europe Solar Store, SunPower SPR-MAX3-400 solar panel | SunPower Solar Module, (n.d.). https://www.europe-solarstore.com/sunpower-spr-max3-400.html (accessed October 18, 2023).
[237] A.P. Borkar, Dr.Ravindra.N. Dehankar, Design and Developments in Different Types of Solar Modified Agricultural Spray Pump: A Review, Int. J. Res. Appl. Sci. Eng. Technol. 10 (2022) 1264–1271. https://doi.org/10.22214/ijraset.2022.42431.
[238] S. Maryani, Rd Kusumanto, Carlos Rs, Solar Panel Optimization Using Peltier Module TEC1-12706, J. Mech. Civ. Ind. Eng. 4 (2023) 43–50. https://doi.org/10.32996/jmcie.2023.4.3.6.
[239] J.E. Bolek, Electrical Concepts in the Surface Electromyographic Signal, Appl. Psychophysiol. Biofeedback 35 (2010) 171–175. https://doi.org/10.1007/s10484-009-9118-x.
[240] P. Silvester, Analysis of LCR Circuits Using Differential Equations Transient and Steady State Solutions, in: Electr. Circuits, Macmillan Education UK, London, 1993: pp. 357–412. https://doi.org/10.1007/978-1-349-10540-3_7.
[241] X. Zhao, R. Cheng, Y. Fu, Heat-collecting performance of linear Fresnel reflector concentrator measuring and forecasting after dust accumulation, Appl. Therm. Eng. 248 (2024) 123321. https://doi.org/10.1016/j.applthermaleng.2024.123321.

[242] A. Nakhaei Zadeh, M. Ameri, A. Shojaei, I. Baniasad Askari, Optical Efficiency of Linear Fresnel Reflectors in Fixed, Variable and Optimal Distance between Mirrors: Theoretical and Experimental Studies, Int. J. Eng. 37 (2024) 283–297. https://doi.org/10.5829/IJE.2024.37.02B.06.
[243] S. Taramona, A. Gallo, H. González-Camarillo, G. Minio Paluello, J.V. Briongos, J. Gómez-Hernández, Beam-down linear Fresnel reflector prototype: Construction and first tests, Renew. Energy 220 (2024) 119697. https://doi.org/10.1016/j.renene.2023.119697.
[244] P. Alamdari, M. Khatamifar, W. Lin, Heat loss analysis review: Parabolic trough and linear Fresnel collectors, Renew. Sustain. Energy Rev. 199 (2024) 114497. https://doi.org/10.1016/j.rser.2024.114497.
[245] A.K. Ramasamy, M. Ganesh, S.S. Kumar, K. Rajamani, Design and performance investigation of modified Hybrid Parabolic Linear Fresnel Collector, Energy Sustain. Dev. 76 (2023) 101273. https://doi.org/10.1016/j.esd.2023.101273.
[246] K. Blume, M. Röger, R. Pitz-Paal, Simplified analytical model to describe wind loads and wind-induced tracking deviations of heliostats, Sol. Energy 256 (2023) 96–109. https://doi.org/10.1016/j.solener.2023.03.055.
[247] Y. Zou, Y. Zhou, Q. Xu, Heliostat Field Layout via Niching and Elite Competition Swarm Optimization, IEEE Access 12 (2024) 31589–31604. https://doi.org/10.1109/ACCESS.2024.3368865.
[248] I. Paul, S.B. Kedare, Determination of optically feasible heliostat field region for solar power tower system employing innovative receiver aperture, Sol. Energy 271 (2024) 112404. https://doi.org/10.1016/j.solener.2024.112404.
[249] A.N. Yerudkar, D. Kumar, V.H. Dalvi, S.V. Panse, V.R. Gaval, J.B. Joshi, Economically feasible solutions in concentrating solar power technology specifically for heliostats – A review, Renew. Sustain. Energy Rev. 189 (2024) 113825. https://doi.org/10.1016/j.rser.2023.113825.
[250] J. Sment, A. Zolan, Status Quo and Gap Analysis of Heliostat Field Deployment Processes for Concentrating Solar Tower Plants, J. Sol. Energy Eng. 146 (2024) 061004. https://doi.org/10.1115/1.4065430.
[251] M. Agha Mohammad Ali Kermani, M. Moghadam, H. Sahebi, S. Rezazadeh Moghadam, Sunlit ventures: maximizing photovoltaic power plant success through strategic investments, Kybernetes ahead-of-print (2024). https://doi.org/10.1108/K-01-2024-0235.
[252] S.O. Salawu, T.A. Yusuf, E.O. Fatunmbi, A.M. Obalalu, Dynamics of tri-hybridized Prandtl-Eyring thermal water-based magneto-nanofuids flow over double stretched wedge sheets experiencing force convection, Forces Mech. 15 (2024) 100270. https://doi.org/10.1016/j.finmec.2024.100270.
[253] K. Praveen, H. Kim, S. Govindarajan, M.W. Lee, Cubic fluorite-based lanthanum cerium oxide thermal barrier top-coat fabrication, properties, and performance: Present status and prospects, J. Eur. Ceram. Soc. 44 (2024) 116804. https://doi.org/10.1016/j.jeurceramsoc.2024.116804.
[254] S.O. Salawu, T.A. Yusuf, A.M. Obalalu, E.O. Fatunmbi, Thermal radiation and propagation of tiny particles in magnetized Eyring–Powell binary reactive fluid with generalized Arrhenius kinetics, Case Stud. Therm. Eng. 58 (2024) 104409. https://doi.org/10.1016/j.csite.2024.104409.
[255] S.O. Salawu, A.M. Obalalu, MD. Shamshuddin, E.O. Fatunmbi, O.J. Ajilore, Thermal stability of magneto-hybridized silicon and aluminum oxides nanoparticle in $C_3H_8O_2$-Williamson exothermic reactive fluid with thin radiation for perovskite solar power, Kuwait J. Sci. 51 (2024) 100284. https://doi.org/10.1016/j.kjs.2024.100284.
[256] J. Yan, Y. Peng, X. Xie, W. Zhou, Optical performance of a solar dish concentrator formed by the same size mirror located on parabolic frame, Sol. Energy Mater. Sol. Cells 275 (2024) 113042. https://doi.org/10.1016/j.solmat.2024.113042.
[257] S. Elhami Joosheghan, P. Rezvani, M. Reza Razfar, Characteristics and improvement of the double-pass electro-chemical discharge machining, Proc. Inst. Mech. Eng. Part B J. Eng. Manuf. (2024) 09544054231222049. https://doi.org/10.1177/09544054231222049.
[258] S.O. Salawu, E.I. Akinola, O.Y. Oludoun, O.M. Ogunlaran, J.A. Akinpelu, Heat radiation absorption and irreversibility of electromagnetic Williamson hybridized $Al2O3{-}CoFe2O4/H2O$ nanofluid: A concentrated power generation, J. Indian Chem. Soc. 101 (2024) 101225. https://doi.org/10.1016/j.jics.2024.101225.
[259] S.O. Salawu, A.M. Obalalu, E.O. Fatunmbi, A.B. Disu, Tiny particles thermal motile in magnetized chemically reacting upper-convective Maxwell stagnation point fluid with radiation, Results Eng. 23 (2024) 102593. https://doi.org/10.1016/j.rineng.2024.102593.
[260] Z. Shi, G. Tang, Y. Lei, H. Gu, L. Gan, Hot corrosion behavior of Co-W coated ferritic stainless steel in molten chloride salt, Surf. Coat. Technol. 480 (2024) 130590. https://doi.org/10.1016/j.surfcoat.2024.130590.
[261] B. Venkateswarlu, S.W. Joo, N. Nagendra, A.S.M. Metwally, Numerical investigation of electromagnetic $[Cu + TiO_2/H_2O]^h$ hybrid nanofluid flow with solar radiation over an exponential stretching surface, Asia-Pac. J. Chem. Eng. n/a (n.d.) e3154. https://doi.org/10.1002/apj.3154.